Catena xxx (xxxx) xxxx

Contents lists available at ScienceDirect

Catena

journal homepage: www.elsevier.com/locate/catena

# Variations of soil $CO_2$ concentration and $pCO_2$ in a cave stream on different time scales in subtropical climatic regime

Min Cao, Yongjun Jiang*, Yu Chen, Jiaxin Fan, Qiufang He

*Chongqing Key Laboratory of Karst Environment & School of Geographical Sciences, Southwest University, Chongqing 400715, China*

ARTICLE INFO

*Keywords:*
Soil $CO_2$-groundwater $pCO_2$
Hydrochemistry
Temperature and precipitation
Principal component analysis

ABSTRACT

In karst regions, soil $CO_2$ is a major chemical driving force for the karst processes and finally has a significant impact on the hydrochemical processes of karst underground river. Hydrochemical features, soil and climatic parameters with a high-temporal resolution have been monitored on different scales (daily scale, seasonal scale and interannual scale, storm scale) in the Xueyu Cave watershed from 2009 to 2015. The aim of this study is to understand how cave stream $pCO_2$ and hydrochemistry respond to overlying soil carbon recharge on different time scales. The results show that the variational amplitudes of the hydrochemistry in Xueyu Cave underground river (XUR) tend to be in the order: storm-scale > seasonal > interannual > daily scale. Soil $CO_2$, $pCO_2$ ($CO_2$ partial pressure in the XUR) and Spc (specific conductivity) were higher in summer and autumn than those in winter and spring. The synchronous variations of XUR $pCO_2$ with soil $CO_2$ concentrations in the same order of magnitude confirm the "soil $CO_2$ effects" on the formation of XUR hydrochemical features. The storm-scale fluctuations of hydrochemistry in XUR water are especially depending on the intensities of rainfalls that determine whether the "dilution effects" or the "$CO_2$ effects" are predominant in the stream during rainfall events. At the same time, soil moisture and soil $CO_2$ work as important factors for controlling $pCO_2$ variations in the XUR. The identified relationship of soil-XUR $pCO_2$ suggests a temperature control on carbonate weathering on daily and seasonal scale but a rainfall/soil moisture control on storm and annual scale. The combined effect of point and diffused infiltration that delays the arrival of storm flows determines the fluctuations of the discharge and $pCO_2$ variation. Defining relationships between $CO_2$ from overlying soils and groundwater offers the chance to explore the processes at different time scales, potentially increasing our ability to understanding the carbon dynamics in karst systems.

## 1. Introduction

Change and increasing concentrations of atmospheric greenhouse gases, not only lead to gradual mean global warming but may also change the frequency, the severity and even the nature of extreme events (IPCC, 2013). Diverse climate-dependent processes occurring on different timescales are involved in ecosystems carbon cycling (Berner, 2003). Karst landscapes provide a natural laboratory to investigate C cycling as C is present in various reservoirs, where the cycling drives development of conduits via calcite dissolution from carbon dioxide ($CO_2$) (Dreybrodt, 1988; Gulley et al., 2013). The subterranean $CO_2$ pool could represent more than half of the total $CO_2$ content of the atmosphere as the non-negligible role of cavities as a temporal depot of $CO_2$ coming from different processes (Serrano-Ortiz et al., 2010). Carbonate weathering and underground $CO_2$ storage are important parts of the terrestrial flux of carbon at different scales (daily to annually) (Liu and Zhao, 2000; Serrano-Ortiz et al., 2010). As $CO_2$ dissolves in water, $H_2CO_3$ that can dissolve any carbonate substrate (e.g. calcite and dolomite) is formed. Soil $CO_2$ serves as a major chemical driving force for carbonate dissolution and has a significant influence on hydrochemical features of karst spring water (Morse and Arvidson, 2002; Ford and Willams, 2007; Liu et al., 2007; Zhao et al., 2010; Yang et al., 2012). For example, variations of air temperature could cause the changes of soil $CO_2$ concentrations by altering the intensity of photosynthesis and respiration of soil organisms, resulting in hydrochemical variations of karst spring water (Liu et al., 2007).

Subsurface caves in the vadose zone always present higher concentration of $CO_2$ than outdoor air. Part of these $CO_2$ fluxes takes place in the overlying soil where $CO_2$ soil diffusion depends on the soil properties and water content (Pu et al., 2014; Pla et al., 2017) and/or the vadose zone, e.g. recent studies have identified an important source of $CO_2$ in caves in the decay of soil organic matter washed down into

* Corresponding author.
*E-mail address:* jiangjyj@swu.edu.cn (Y. Jiang).

https://doi.org/10.1016/j.catena.2019.104280
Received 8 June 2018; Received in revised form 11 August 2019; Accepted 19 September 2019

the unsaturated zone (Mattey et al., 2016). The $CO_2$ stored in caves commonly presents $CO_2$ variations strongly driven by ventilation that is regulated by synoptic weather conditions (Kowalczk and Froelich, 2010; Fernandez-Cortes et al., 2011; Frisia et al., 2011; Yang et al., 2012). Moreover, advection movement that is determined by air density and cave geometry has been observed to be an important mechanism of $CO_2$ transport throughout some underground environments (Frisia et al., 2011; Faimon et al., 2012; Mattey et al., 2016). Rainfall and the relative humidity of air regulate the water content in soil and host rock porous media controlling gas exchange between the surface and underground (Cuezva et al., 2011). The arrival of freshly filtrated rainwater at a karst spring can thus be recognized by changing water temperature and decreasing specific electric conductivity (Ford and Willams, 2007). Karst springs and karst aquifers typically show marked and rapid reactions to precipitation events in both water quantity and quality variables. Therefore, monitoring at high temporal resolutions, ideally continuous monitoring, is required to characterize the dynamic behavior and variability of karst systems (Hartmann et al., 2014).

It has been found that hydrochemical features of karst springs show variations on different time scales, including diurnal (de Montety et al., 2011; Jiang et al., 2013; Pu et al., 2014), seasonal and storm-scale variations (Liu et al., 2007; Pu et al., 2014; Li et al., 2016; Cholet et al., 2017). Abrupt changes in the hydrochemistry of the karst spring water in response to rainfall events are well documented by previous studies (Hess and White, 1988; Quinlan and Alexander, 1987; Ryan and Meiman, 1996; Vesper and White, 2004; Liu et al., 2007; Li et al., 2016). "Soil $CO_2$ effect" with an increase in $pCO_2$ and Spc, and "dilution effect" with a decrease in pH and Spc are alternatively dominant in the karst underground flow (Quinlan and Alexander, 1987; Yang et al., 2012). $CO_2$ concentrations in karstic cavities show significant seasonal (Spötl et al., 2005; Fernandez-Cortes et al., 2011; Pla et al., 2016) and even daily variations (Baldini et al., 2008; Kowalczk and Froelich, 2010). After rainfall events, infiltrating water dissolves the soil $CO_2$, acting as a geochemical $CO_2$ sink by reducing the $CO_2$ emissions and percolates downward (Serrano-Ortiz et al., 2010).

In this study, an extensive study of soil temperature, soil water content, soil $CO_2$ and the pH, water temperature and Spc with high-temporal resolution (every 15 min) monitoring has been conducted at Xueyu Cave, a typical karst watershed, Chongqing, SW China (Fig. 1), to understand $CO_2$ variations of soil and underlying cave stream at different scales in a detailed field study and to find out major controlling factors that are responsible for the $pCO_2$ variations in the XUR, to understand the biogeochemical processes that regulate the soil $CO_2$ flux. Overall, the aim of the present research is to characterize processes involved in $CO_2$ exchange in the underground stream-soil system at the diel/seasonal/annual and rainfall scale.

## 2. Study area

Cave karst underground river (XUR) system (latitude 29°47′00″ N, longitude 107°47′13″ E; altitude 233 m a.s.l.) with an area of 13 $km^2$ is located on the left bank of Long River (a tributary of the Yangtze River), SE of Fengdu county, Chongqing, Southwest China (Fig. 1). The XUR is developed in the Triassic Feixianguan Formation ($T_{1f}$), which consists of limestone with a thickness of 150–250 m (Huang et al., 2008) with sedimentary environment of evaporate-carbonate platform (Zharkov and Chumakov, 2001). The geological structure of Xueyu Cave is characterised by the existence of NE-SW monocline. Karst landforms are well developed at the surface of the carbonate outcrops, mainly in the Triassic limestones located at higher altitudes, including dolines, karst swallow holes and cave systems (Fig. 1). Evidence of hypogenic (deep, confined) speleogenesis has not been detected. Overlying soils are mainly the zonal yellow soil, of which the thickness is heterogeneous, varying from 20 cm to 50 cm.

The regional climate is characterized by a humid subtropical monsoon climate with the average annual precipitation of 1100 mm (over 70% of precipitation occurring during the rainy season from May to October) and the mean annual air temperature of 16.5 °C. The air temperature and precipitation in the study area vary in a consistent manner, both being high in the wet season and low in the dry season except when it is dominated by the subtropical high-pressure belt in July and August. Precipitation is the only recharge source to the aquifer and discharge is through cave systems. Previous investigations by Zhu et al. (2004) and Pu et al. (2016) have described the hydrogeological and hydrochemical functioning of the Xueyu Cave. The vegetation is mainly composed of evergreen, broad-leaf forests and shrubs. The land use types are mainly forest and dry lands reclaimed from grain plots. The vegetation is mainly composed of evergreen, broad-leaf forests and shrubs. There are no mining or industrial plants around and the population in the watershed is 500.

The underground river is the only entrance of Xueyu Cave with an explored length of 1644 m. The mean annual air temperature in the cave is 17.2 °C and the humidity from 76.7% to 100%. The discharge of the underground river ranges from 4.1 l/s in dry period to 26.6 l/s in wet period. Most parts of the cave are narrow, deep passages (canyon passages), which are developed along strata. The cave can be divided into three broad levels at 233–236 m (Level I), 249–262 m (Level II) and 281–283 m. (Level III) above sea level (Fig. 2). The modern stream flows only in the bottom level (Pu et al., 2016). There is no allogenic stream sinking underground at the head of Xueyu Cave (Pu et al., 2015).

## 3. Materials and methods

### 3.1. Automatic data logging

A MS-5 multi-channel water quality multiprobe (made by Hach Corporation, U.S.A) was placed at the outlet of the Xueyu Cave XUR to obtain continuous hydrochemical variations from January 2009 to December 2015. The information of specific equipment and related precision were listed in Table 1. Also, a GMP22 carbon dioxide probe of VALSALA with waterproof films was placed to measure $p_{CO_2}$ from October 2014. The soil temperature and soil $CO_2$ concentrations were obtained from May 2013 by a composite measurement system, including a $CO_2$ sensor (GMP22, made by VAISALA in Finland) and temperature sensor (AV-10T, produced by AVALON, U.S.A) that were imbedded into the soil at the depth of 40 cm by drilling in the soil sampling site which is located about 40 m on the top with an elevation of about 300 m a.s.l. and 400 m in horizontal distance from the entrance of the cave (Fig. 2). The main species of vegetation in the surrounding of the soil profile are the broad-leaf woods with dominant *Broussonetia papyrifera* and *Cercis chinensis Bunge*. The data of air temperature and precipitation were obtained by HOBO field weather stations since January 2009, located near the cave entrance. All the data loggers (the water quality, $CO_2$ measurement system and weather data) were set to monitor the synchronous changes at the same time-interval of 15 min.

The sensors and probes were calibrated prior to deployment. A $CO_2$ portable analyzer (GM70, made in Finland) and hand-held water quality meter (WTW350i, made in Germany) were used monthly to check the reliability of automatic and continuous measurements. The discharge of XUR was calculated based on the monitoring of water level and the measurement of a flowmeter.

### 3.2. In situ titration and major ion analysis

[$HCO_3^-$] and [$Ca^{2+}$] were measured monthly on the site using the Aquamerck alkalinity test kit and the hardness test kit (Table 1). Water samples were filtered through 0.45 μm Millipore filters into 100 ml acid-washed high-density polyethylene bottles for ion analyses. Samples for cation test were acidified to pH < 2.0 by using concentrated nitric acid to prevent complexation and precipitation. The samples were taken back to the laboratory to determine cation concentrations of $Na^+$,

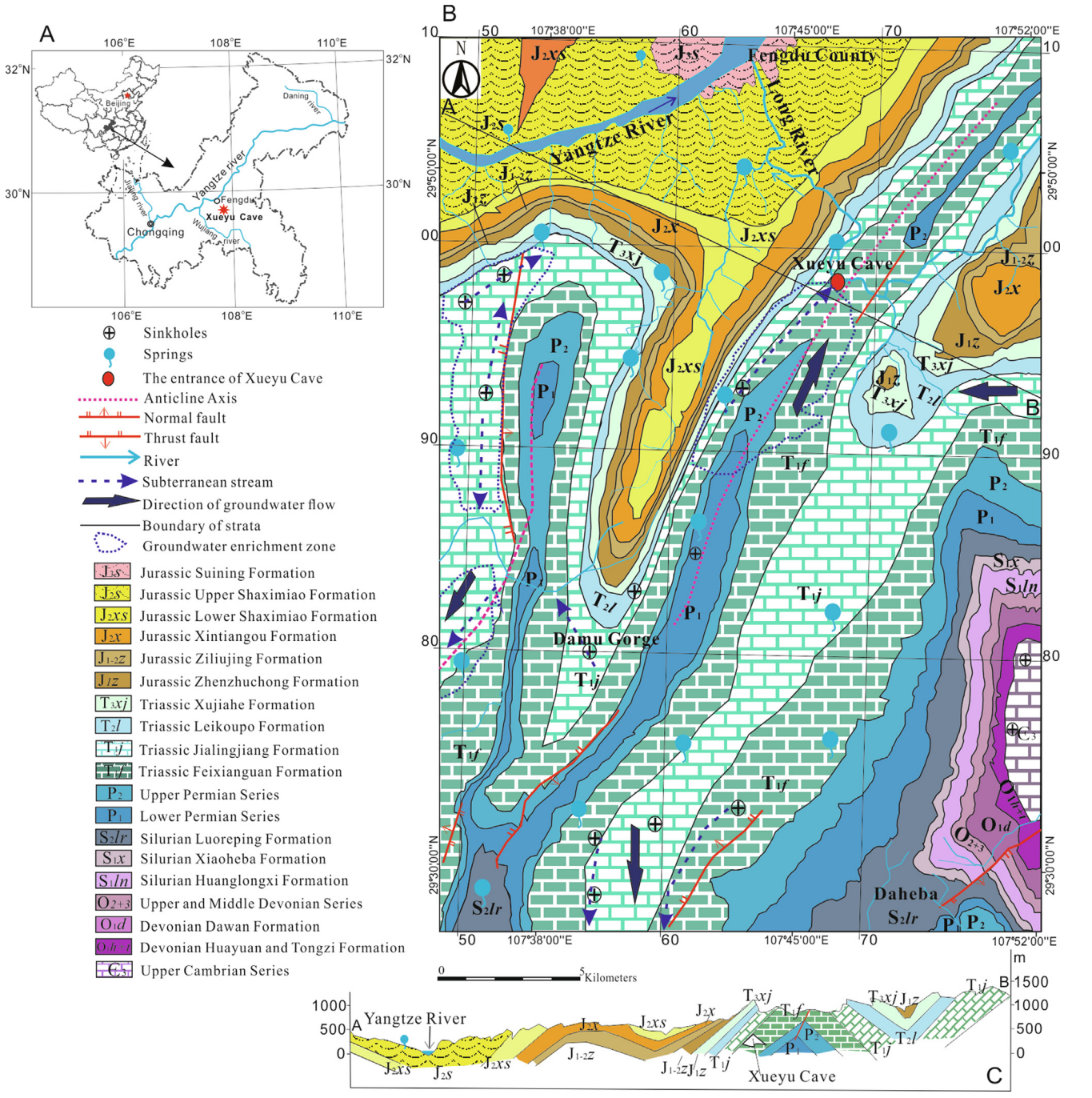


**Fig. 1.** Location, geological setting and geological cross section in the Xueyue Cave watershed (Modified from Wu et al. (2015)).

$K^+$ and $Mg^{2+}$ by inductively coupled plasma optical emission spectrometer (ICP-OES) and anion concentrations of $SO_4^{2-}$, $Cl^-$ and $NO_3^-$ by ion chromatography. Precisions of all ion analyses were $< 0.1$ mg/l.

### 3.3. Calculation of $pCO_2$ and SIc

The $pCO_2$ and calcite saturation index (SIc) in the XUR are related to its calcium, and bicarbonate concentrations, pH and temperature, which are important indexes in the karst groundwater.

$$pCO_2 = \frac{[HCO_3^-][H^+]}{K_H K_1}$$

where $K_H$ and $K_1$ are the temperature dependent Henry's Law and first dissociation constants for $CO_2$ gas in water, respectively (Wigley, 1977)

$$SIc = lg\left[\frac{[Ca^{2+}][CO_3^{2-}]}{K_c}\right]$$

where $K_c$ is the temperature-dependent equilibrium constant for calcite (Stumm and Morgan, 1981).

In the karst watershed, the compositions of underground river water are dominated by the dissolution of carbonate rocks. Thus, $Ca^{2+}$ and $Mg^{2+}$ are the major cations and $HCO_3^-$ is the major counterbalancing anion in the XUR. Consequently, these ions dominate the Spc, to which their concentrations are directly proportional. As the Spc is directly and continuously measured, this feature is used to estimate $Ca^{2+}$ and $HCO_3^-$ concentrations. For this purpose, the linkages between ion concentrations and Spc was established from the monthly spot-sampled data (Fig. 3):

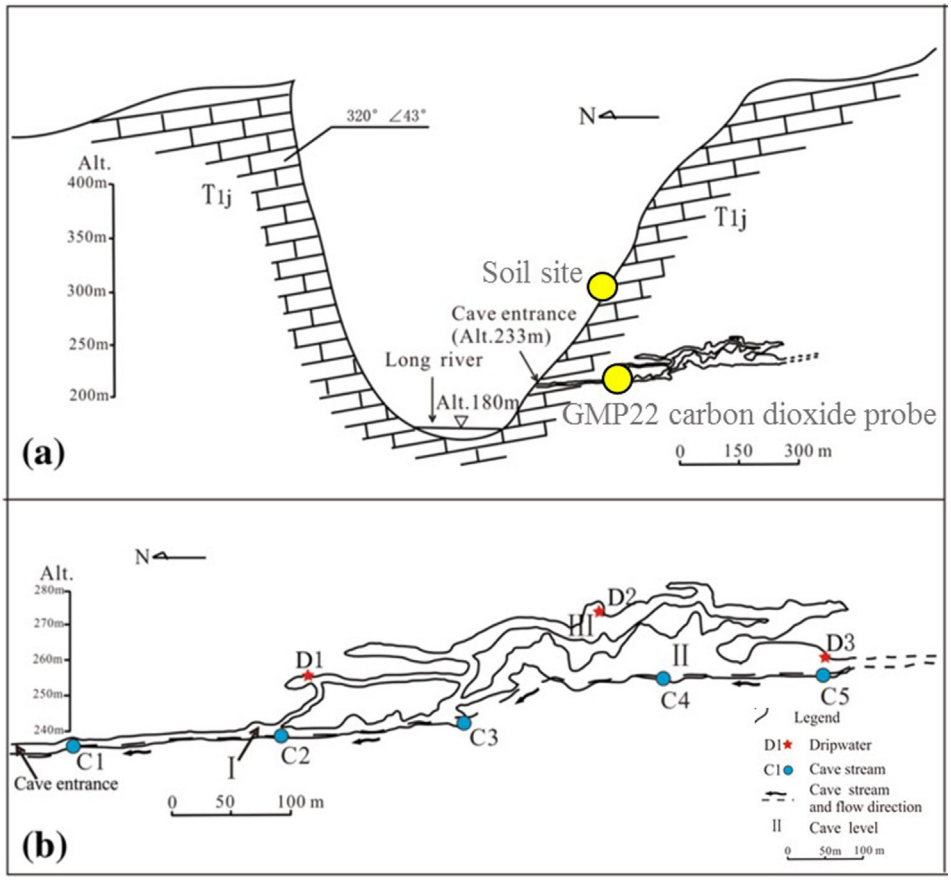


**Fig. 2.** (a) Areal profile and (b) General sketch of Xueyu Cave passages, Chongqing, SW China (Pu et al., 2016).

**Table 1**
Continuous monitoring items, related equipment name and the precision.

| Equipment | Monitoring items | Precision |
|---|---|---|
| Water quality multiprobe | Water temperature | 0.1 °C |
| | pH | 0.01 pH units |
| | Water level | 0.01 cm |
| | Spc | 1 μS/cm |
| GMP22 carbon dioxide probe | $pCO_2$ | 1 ppm |
| | Soil $CO_2$ | 1 ppm |
| AV-10 T | Soil temperature | 0.1 °C |
| HOBO field weather stations | Air temperature | 0.1 °C |
| | Precipitation | 0.01 mm |
| Aquamerck alkalinity test kit | $[HCO_3^-]$ | 0.1 mmol/l |
| Hardness test kit | $[Ca^{2+}]$ | 1 mg/l |
| ICP-OES | $Na^+$, $K^+$, $Mg^{2+}$ | 0.01 mg/l |
| Ion chromatography | $SO_4^{2-}$, $Cl^-$, $NO_3^-$ | 0.01 mg/l |

$$[Ca^{2+}] = 0.25 \times Spc - 9.06;\ R^2 = 0.96$$
$$[HCO_3^-] = 0.68 \times Spc - 22.12;\ R^2 = 0.97$$

where brackets denote species concentrations in mg/l and Spc in μS/cm at 25 °C.

### 3.4. Principal component analysis (PCA)

PCA is a method of statistics for information extraction, which can help to find out the combination of variables that are not correlated (P), but corresponding to one principal component, that is, the main control factor for variables that distribute differently in each factor.

Fp = a1i ∗ ZX1 + a2i ∗ ZX2 + ·····+api ∗ ZXp

*a1i, a2i, ....., api (i = 1,....., m) are eigenvectors that are consistent with eigenvalues of X's covariance, ZX1, ZX2, ....., ZXp are

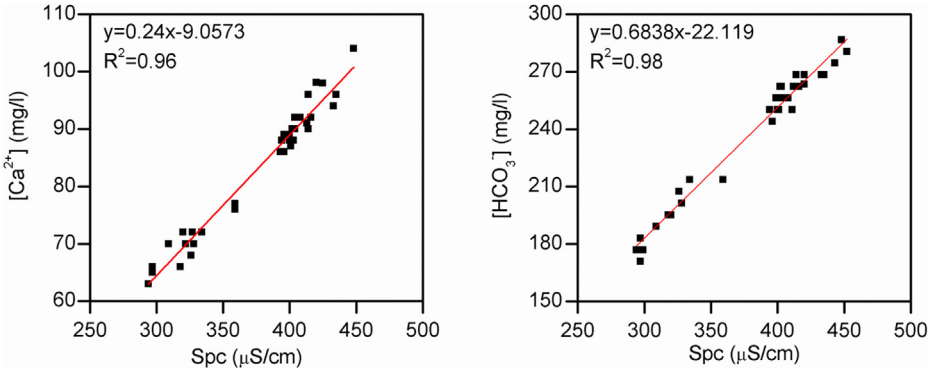


**Fig. 3.** The relationship between Spc vs. $Ca^{2+}$ and Spc vs. $HCO_3^-$ concentrations of Xueyu Cave karst underground river water.

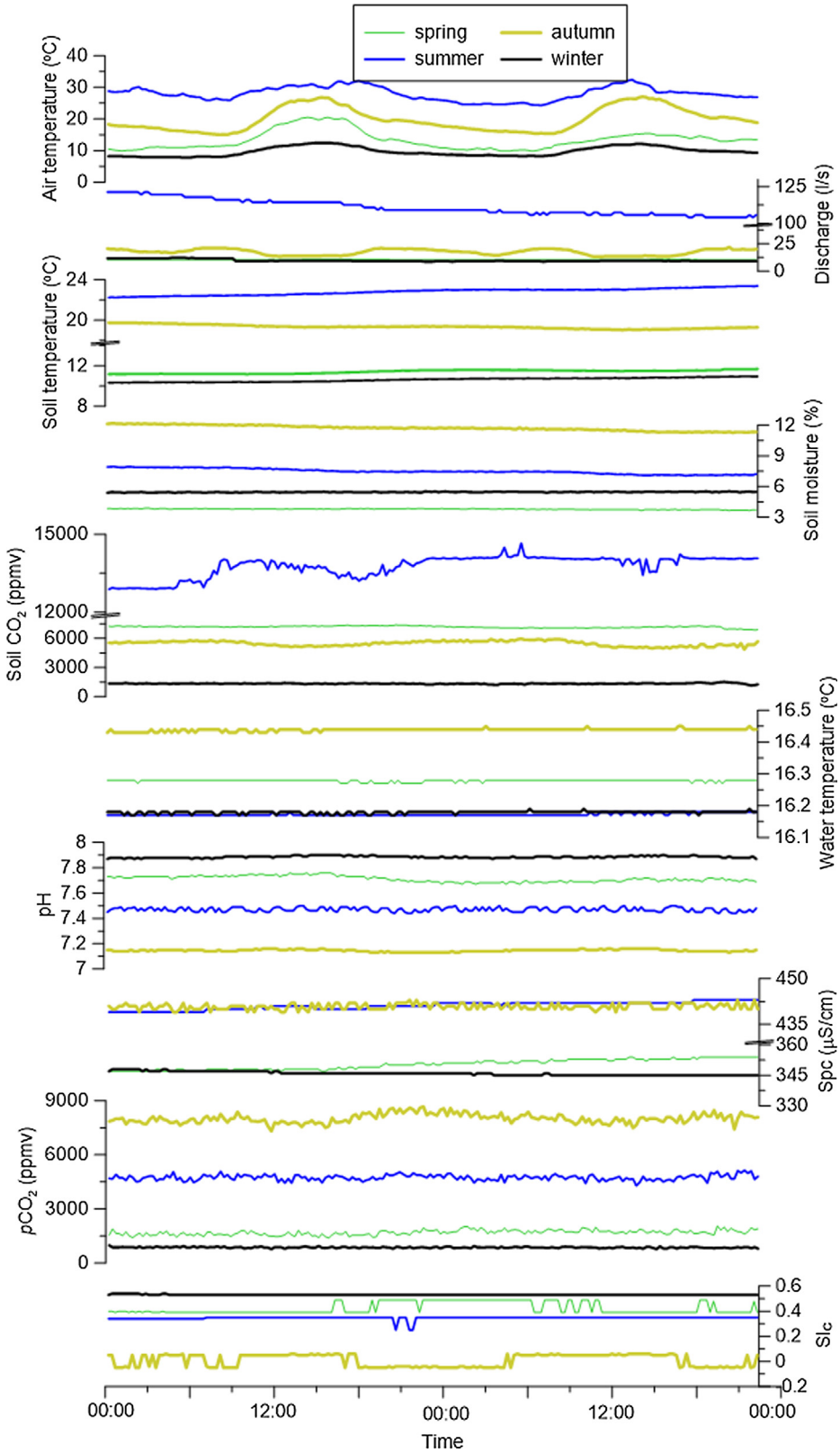


**Fig. 4.** Diel variations of the KUR hydrochemistry, air/soil/groundwater temperatures and soil moisture/$CO_2$ in Xueyu Cave watershed based on two-day monitoring occurred in different seasons (8th-9th, March; 24th-25th, June; 14th-15th, October; 29th-30th, December).

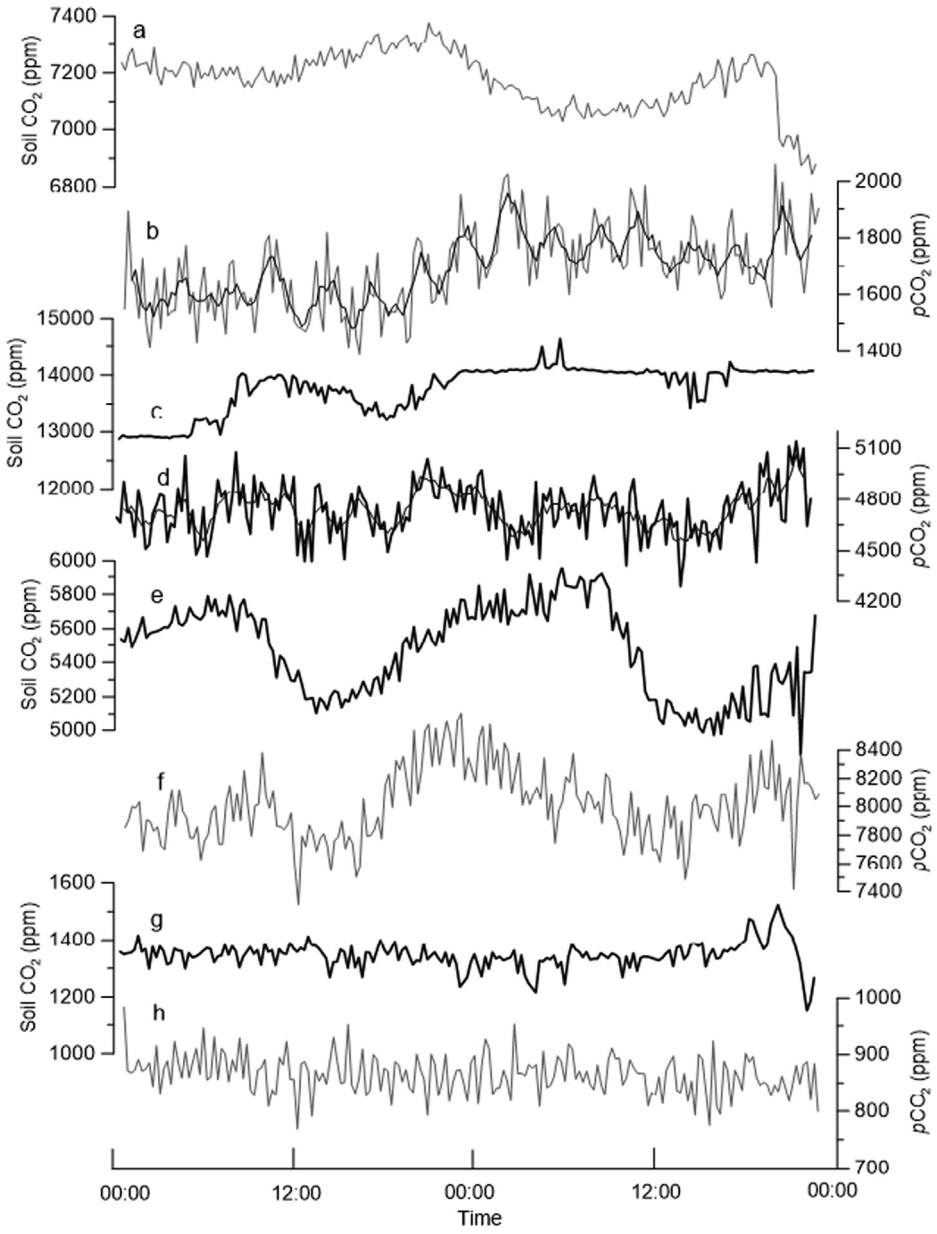


**Fig. 5.** The daily co-variation of soil $CO_2$ concentrations and $pCO_2$ in the XUR (amplified the parts from Fig. 4, a, c, e, g and b, d, f, h refers to daily variation of soil $CO_2$ and $pCO_2$ in spring, summer, autumn and winter, respectively).

standardized values from original variables. The results were obtained from SPSS V21.0.

## 4. Results

### 4.1. Soil-Cave physicochemical parameters outside of the cave from daily to annual scales

The air temperature showed significant daily and seasonal changes in the Xueyu Cave watershed (Figs. 4–6). Besides, the magnitudes of daily variations in air temperature were higher in spring/autumn (10.7/11.9 °C) than in summer/winter (8.1/4.6 °C). The seasonal air temperature ranged from 10.5 to 25.6 °C with a mean value of 18.8 ± 6.4 °C. The seasonal soil temperature ranged from 13.5 to 22.3 °C with a mean value of 17.9 ± 4.1 °C, which is very close to the air temperature range (Table 2). But the daily soil temperature variability was only slightly changed (0.5–1.1 °C). The daily variations of soil moisture ranged from 0.2% to 0.9% under conditions without precipitation (Fig. 4). The relationship between soil moistures and soil temperatures was negatively correlated in summer ($R^2 = 0.90$, $p < 0.01$), but positively correlated in autumn ($R^2 = 0.78$, $p < 0.01$). The daily variations of soil $CO_2$ concentration were in the range of 370–1776 ppm, following the order: summer > autumn > spring > winter days (Table 2). Differences in the amplitude of daily variation in summer and winter were significant, but in autumn, daily patterns of soil $CO_2$ concentration were characterized by symmetrical cycles (Fig. 5). Their seasonal variations ranged from 1346 ppm in winter to 13769 ppm in summer (Fig. 6). The soil parameter monitoring only lasted for 2 years, not available for annual-scale analysis.

The water temperature of the XUR changed a little (less than 0.3 °C) no matter on daily, seasonal or annual scales (Table 2). The daily variational magnitudes of discharge ranged from 0.5 to 17.3 l/s without rainfall events. While on a seasonal scale it ranged from 8.7 l/s in winter to 29.6 l/s in summer, but from 15.4 l/s to 27.1 l/s over the annual scale. Spc showed daily variability of 2–7 μS/cm, seasonal variability of 374–425 μS/cm and the annual variability of 384–418 μS/

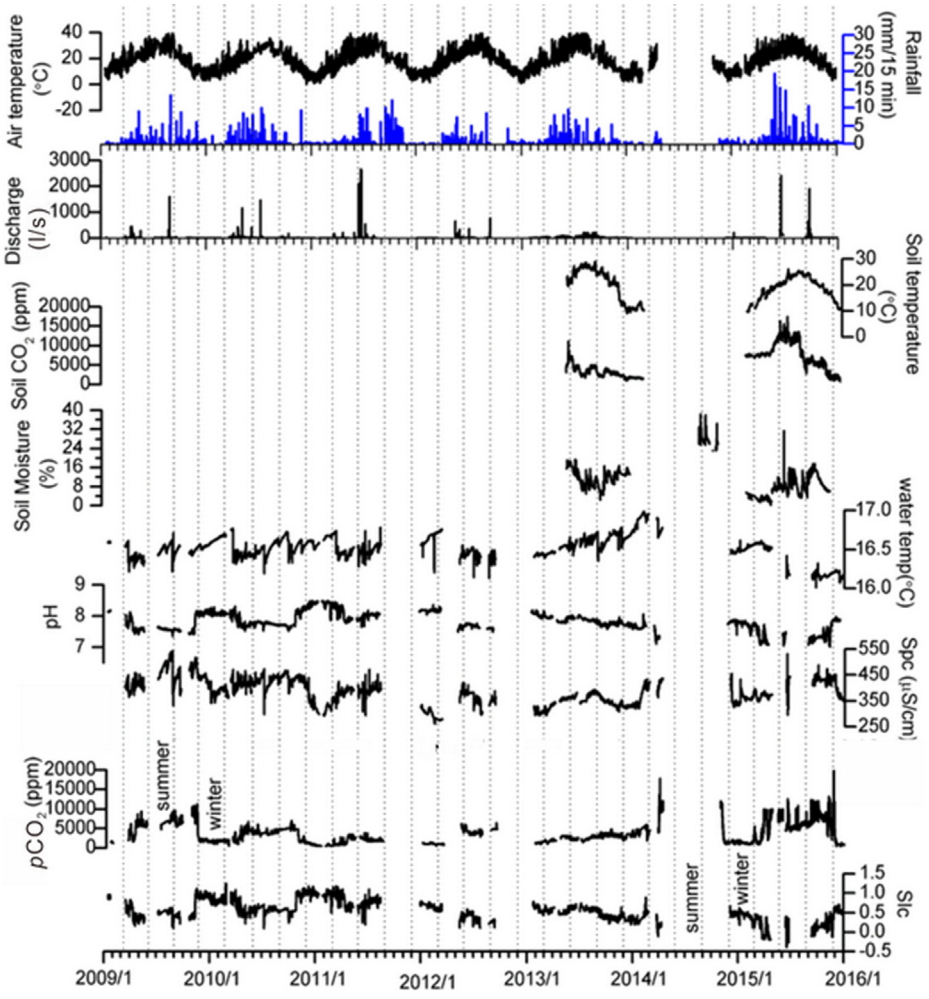


**Fig. 6.** Continuous variations of the XUR hydrochemistry and environmental variables from 2009 to 2015.

cm. The daily variability of $pCO_2$ in the XUR water was from 225 ppm to 1355 ppm, which was the most diverse physiochemical variable in the water. The difference in amplitudes of daily variations between soil and XUR $pCO_2$ was very similar though daily dynamics was less distinctive in the stream $pCO_2$ than in soil $CO_2$. The seasonal patterns of $pCO_2$ variations in XUR were also pronounced (Table 3). Stream water was always oversaturated (SIc > 0) under the condition of no precipitation, which showed lower values in summer and oversaturated values in winter. The daily variability of pH was less than 0.1 pH unit. pH values were higher in dry season than in wet season, ranging from 7.5 to 8.1; the annual pH values tended to show a declining trend (Table 4). DIC and $Ca^{2+}$ were the two main ions in the stream, which accounting for about 90% of all ions. They changed slightly on a daily scale, from 2.0 to 4.7 mg/l and from 0.6 to 1.7 mg/l for DIC and $Ca^{2+}$; they also showed significant seasonal patterns, 234.8–272.2 mg/l and 76.6–98.8 mg/l for DIC and $Ca^{2+}$, respectively. Seasonal $NO_3^-$ and $SO_4^{2-}$ concentrations ranged from 3.1 mg/l to 3.6 mg/l, from 7.8 mg/l to 22.6 mg/l, respectively (Table 3). $Cl^-$ concentrations were within the ranged of 0.1 to 3.5 mg/l. $K^+$ and $Na^+$ concentrations were from 0.5 mg/l to 1.2 mg/l. $Mg^{2+}$ concentrations ranged from 1.2 to 2.0 mg/l. On an annual scale, the air temperature, precipitation, discharge, water temperature and XUR $pCO_2$ showed a clearly increasing trend while pH, Spc, DO, DIC and SIc showed a decreasing trend. $K^+$, $Na^+$, $NO_3^-$ and $SO_4^{2-}$ concentrations were slightly increased (Table 4).

### 4.2. Responses of soil-cave physicochemical parameters to rainfall events

Figs. 7–9 showed the dynamic monitoring results in XUR system during the rainfall processes (light rain, moderate rain and rainstorm). During the light rain (Table 2), the diel variational magnitude of air temperature was about 15.6 °C, which dropped rapidly from 25.8 °C to 17.8 °C within 1 h after the light rain event, causing the collapse of the daily temperature patterns. The soil temperature reduced about 0.5 °C. While during the moderate and heavy storm, soil temperatures reduced by 1.5 °C. The soil moisture changed largely, from 2.1% during the light rain to 22.5% during the storm. The soil $CO_2$ concentrations declined at the beginning of the rainfall events, but increased after the rain. The variational magnitudes ranged from 400 ppm to 3000 ppm.

The XUR discharge was nearly unchanged (< 1.0 l/s) during the light rain. However, during a storm, the discharge could increase above 2000 l/s (Table 2). Stream water temperatures increased after moderate and storm events, showing correspondence with variations of rainfall intensity. The pH variability was less than 0.1 during the light rain, but decreased 0.5 pH units under a storm event as the “dilution effect” occurred. The Spc variation was slightly increased during the light rain, it rose by 73 μS/cm during the moderate rain but declined by 143 μS/cm during a storm. The $pCO_2$ in XUR fluctuated about 800 ppm during a light rain, but increased by 6750 ppm during the storm processes. The SIc, concentrations of $K^+$, $Na^+$, $Ca^{2+}$, $Mg^{2+}$, $HCO_3^-$ in XUR water tended to increase during the moderate rain due to the “soil $CO_2$ effect” and decrease during the storm events, showing synchronous variation with Spc.

**Table 2**
Daily, seasonal and annual variations of air temperature, soil parameters and physicochemical parameters of Xueyu system.

| | Daily scale | | | | Seasonal scale | Annual scale | Rainfall scale | | |
|---|---|---|---|---|---|---|---|---|---|
| | Spring | Summer | Autumn | Winter | | | Little rain | Moderate rain | Storm |
| **Air Temp (°C)** | | | | | | | | | |
| Range | 9.8–20.5 | 24.3–32.4 | 15.0–26.9 | 7.8–12.4 | 10.5–25.6 | 18.2–19.7 | 17.5–33.2 | 19.4–20.8 | 21.1–27.5 |
| Mean | 13.3 ± 2.9 | 28 ± 2.2 | 19.9 ± 3.7 | 9.7 ± 1.5 | 18.8 ± 6.4 | 18.8 ± 0.5 | 24.7 ± 4.2 | 20.0 ± 0.3 | 23.1 ± 1.6 |
| **Soil Temp (°C)** | | | | | | | | | |
| Range | 11.2–11.7 | 22.3–23.4 | 19.0–19.7 | 10.3–11.0 | 13.5–22.3 | 16.4–16.5 | 18.4–18.8 | 21.1–21.9 | 20.2–21.4 |
| Mean | 11.4 ± 0.2 | 22.8 ± 0.3 | 19.4 ± 0.2 | 10.6 ± 0.3 | 17.9 ± 4.1 | 16.5 ± 0.1 | 18.6 ± 0.1 | 21.5 ± 0.2 | 20.6 ± 0.3 |
| **Soil Moisture (%)** | | | | | | | | | |
| Range | 3.6–3.8 | 7.1–7.9 | 11.3–12.2 | 5.4–5.5 | 1.8–18.7 | – | 2.8–4.3 | 12.1–16.1 | 9.4–31.5 |
| Mean | 3.8 ± 0.1 | 7.5 ± 0.9 | 11.7 ± 0.9 | 5.5 ± 0.00 | 11.3 ± 4.0 | – | 3.5 ± 0.3 | 13.5 ± 1.5 | 10.9 ± 3.4 |
| **Soil $CO_2$ (ppm)** | | | | | | | | | |
| Range | 6843–7377 | 12876–14652 | 4858–5958 | 1154–1524 | 1346–13769 | – | 7729–8112 | 5706–6175 | 12672–15611 |
| Mean | 7174 ± 534 | 13769 ± 1776 | 5474 ± 1100 | 1346 ± 370 | 7425 ± 3403 | – | 7989 ± 81 | 5915 ± 93 | 13893 ± 1052 |
| **$pCO_2$ (ppm)** | | | | | | | | | |
| Range | 1388–2060 | 4287–5141 | 7310–8665 | 769–984 | 861–7972 | 2679–5566 | 7504–8310 | 6968–11920 | 5833–12580 |
| Mean | 1692 ± 678 | 4739 ± 854 | 8013 ± 1355 | 865 ± 215 | 5372 ± 1368 | 3937 ± 874 | 7856 ± 165 | 8693 ± 1760 | 9604 ± 2420 |
| **pH** | | | | | | | | | |
| Range | 7.7–7.8 | 7.4–7.5 | 7.1–7.2 | 7.8–7.9 | 7.5–8.1 | 7.5–8.0 | 7.1–7.2 | 7.0–7.2 | 7.1–7.4 |
| Mean | 7.7 ± 0.1 | 7.5 ± 0.1 | 7.2 ± 0.1 | 7.9 ± 0.1 | 7.8 ± 0.2 | 7.8 ± 0.1 | 7.2 ± 0.1 | 7.1 ± 0.1 | 7.2 ± 0.1 |
| **SIc** | | | | | | | | | |
| Range | 0.39–0.49 | 0.25–0.35 | −0.05–0.06 | 0.53–0.54 | 0.41–0.72 | 0.32–0.71 | −0.10—0.09 | −0.19—0.01 | −0.35–0.28 |
| Mean | 0.42 ± 0.05 | 0.35 ± 0.01 | 0.01 ± 0.05 | 0.53 ± 0.00 | 0.55 ± 0.11 | 0.57 ± 0.12 | −0.10 ± 0 | −0.13 ± 0.05 | −0.11 ± 0.14 |
| **Discharge (l/s)** | | | | | | | | | |
| Range | 10.3–10.8 | 104.0–121.3 | 13.1–21.9 | 8.6–12.2 | 8.7–29.6 | 15.4–27.1 | 13.2–13.8 | 16.5–670.4 | 183.0–2426.5 |
| Mean | 10.4 ± 0.2 | 110.9 ± 5.2 | 17.3 ± 2.7 | 9.7 ± 1.1 | 20.2 ± 7.8 | 20.2 ± 3.2 | 13.4 ± 0.3 | 96.4 ± 159.1 | 663.1 ± 653.6 |
| **Spc (μS/cm)** | | | | | | | | | |
| Range | 347–354 | 439–441 | 439–443 | 345–348 | 374–425 | 384–418 | 369–372 | 388–461 | 310–453 |
| Mean | 350.4 ± 2.5 | 440.1 ± 1.3 | 440.8 ± 1.0 | 345.9 ± 0.9 | 397.9 ± 18.1 | 397.0 ± 13.2 | 370.0 ± 1.1 | 404.2 ± 19.3 | 359.4 ± 23.1 |
| **DIC (mg/l)** | | | | | | | | | |
| Range | 215.2–219.9 | 258.0–260.8 | 278.1–280.8 | 213.8–215.8 | 234.8–272.2 | 240.3–263.8 | 230.2–232.2 | 243.2–293.1 | 189.9–287.6 |
| Mean | 217.5 ± 1.7 | 259.5 ± 0.8 | 279.3 ± 0.7 | 214.3 ± 0.6 | 251.5 ± 13.5 | 249.3 ± 8.7 | 230.9 ± 0.7 | 253.8 ± 13.3 | 223.2 ± 15.8 |
| **$Ca^{2+}$ (mg/l)** | | | | | | | | | |
| Range | 76.0–77.7 | 91.5–92.5 | 98.5–99.5 | 75.5–76.2 | 76.6–98.9 | 85.0–93.4 | 81.1–82.1 | 86.04–103.9 | 66.9 ~ 102.0 |
| Mean | 76.8 ± 0.6 | 92.1 ± 0.3 | 99.0 ± 0.3 | 75.7 ± 0.2 | 88.3 ± 8.1 | 88.2 ± 3.1 | 81.6 ± 0.3 | 89.8 ± 4.8 | 78.8 ± 5.7 |

**Table 3**
Seasonal variations of hydrochemical parameters in Xueyu stream.

| | Water T (°C) | pH | Spc (μS/cm) | Discharge (l/s) | $pCO_2$ (ppm) | DO (mg/l) | $K^+$ (mg/l) | $Na^+$ (mg/l) | $Mg^{2+}$ (mg/l) | $Ca^{2+}$ (mg/l) | $HCO_3^-$ (mg/l) | $NO_3^-$ (mg/l) | $SO_4^{2-}$ (mg/l) | $Cl^-$ (mg/l) |
|---|---|---|---|---|---|---|---|---|---|---|---|---|---|---|
| Spring | 16.2 | 7.6 | 428.0 | 24.2 | 6607 | 9.3 | 0.5 | 0.8 | 1.2 | 92.0 | 243.8 | 3.5 | 22.0 | 1.8 |
| Summer | 16.3 | 7.6 | 406.0 | 29.6 | 6050 | 9.0 | 0.5 | 0.8 | 2.0 | 98.0 | 258.7 | 3.1 | 16.7 | 3.5 |
| Autumn | 16.5 | 7.3 | 448.0 | 18.3 | 7972 | 8.3 | 0.7 | 1.2 | 1.8 | 108.0 | 305.0 | 3.2 | 7.8 | 0.1 |
| Winter | 16.2 | 8.0 | 355.0 | 8.7 | 861 | 9.9 | 0.5 | 1.0 | 1.9 | 88.0 | 237.9 | 3.6 | 15.2 | 2.6 |

**Table 4**
Annual variations of hydrochemical parameters in Xueyu stream.

| Year | Air T (°C) | Water T (°C) | Precipitation (mm) | Discharge (l/s) | pH | SIc | Spc (μS/cm) | $pCO_2$ (ppm) | $Ca^{2+}$ (mg/l) | $K^+$ (mg/l) | $Na^+$ (mg/l) | $Mg^{2+}$ (mg/l) | $HCO_3^-$ (mg/l) | $Cl^-$ (mg/l) | $NO_3^-$ (mg/l) | $SO_4^{2-}$ (mg/l) |
|---|---|---|---|---|---|---|---|---|---|---|---|---|---|---|---|---|
| 2009 | 18.8 | 16.5 | 903 | 20.2 | 7.8 | 0.6 | 418 | 4562 | 93.4 | 0.6 | 0.9 | 2.3 | 263.8 | 7.6 | 1.9 | 17.5 |
| 2010 | 18.4 | 16.5 | 740 | 15.4 | 7.9 | 0.7 | 413 | 3104 | 92.1 | 0.6 | 0.7 | 1.9 | 260.2 | 7.7 | 1.7 | 18.5 |
| 2011 | 18.8 | 16.5 | 938 | 19.0 | 8.0 | 0.7 | 386 | 2679 | 85.5 | 0.5 | 2.3 | 2.4 | 241.8 | 8.1 | 2.3 | 16.9 |
| 2012 | 18.2 | 16.5 | 986 | 19.1 | 7.8 | 0.5 | 384 | 3781 | 85.0 | 0.5 | 4.4 | 2.2 | 240.3 | 7.9 | 2.7 | 14.6 |
| 2013 | 19.7 | 16.5 | 874 | 20.2 | 7.8 | 0.6 | 397 | 3937 | 88.3 | 0.5 | 1.3 | 1.9 | 249.6 | 7.5 | 3.5 | 14.2 |
| 2014 | 18.4 | 16.5 | 1049 | 20.2 | 7.8 | 0.5 | 395 | 3931 | 87.8 | 0.5 | 0.9 | 2.1 | 248.1 | 6.2 | 3.3 | 24.7 |
| 2015 | 19.2 | 16.5 | 1150 | 27.1 | 7.5 | 0.3 | 385 | 5566 | 85.4 | 0.5 | 0.7 | 2.1 | 241.3 | 5.8 | 3.2 | 22.3 |

### *4.3. PCA analysis of XUR hydrochemistry on different time scales*

With respect to the variations of parameters examined in the soils and water from the XUR system, the variability of these parameters tends to be storm-scale > seasonal > interannual > diel scale. The main controlling factors for the variations of $pCO_2$ on different time scales were revealed by principal component analysis (PCA) (Table 5). $Ca^{2+}$ and $HCO_3^-$ are highly correlated to Spc. Due to this fact, we omitted $Ca^{2+}$ and $HCO_3^-$, and only used Spc in the PCA analysis. On an annual scale, as the limited monitoring data, there were no insufficient data for PCA analysis. Three or four principal components or factors explaining 75% of the variance were extracted.

### *4.4. Calculation of carbon sink*

Based on high-resolution monitoring, it is possible to calculate the carbon that is dissolved in the karst water in the form of dissolved inorganic carbon (DIC) from the atmosphere by the water-rock

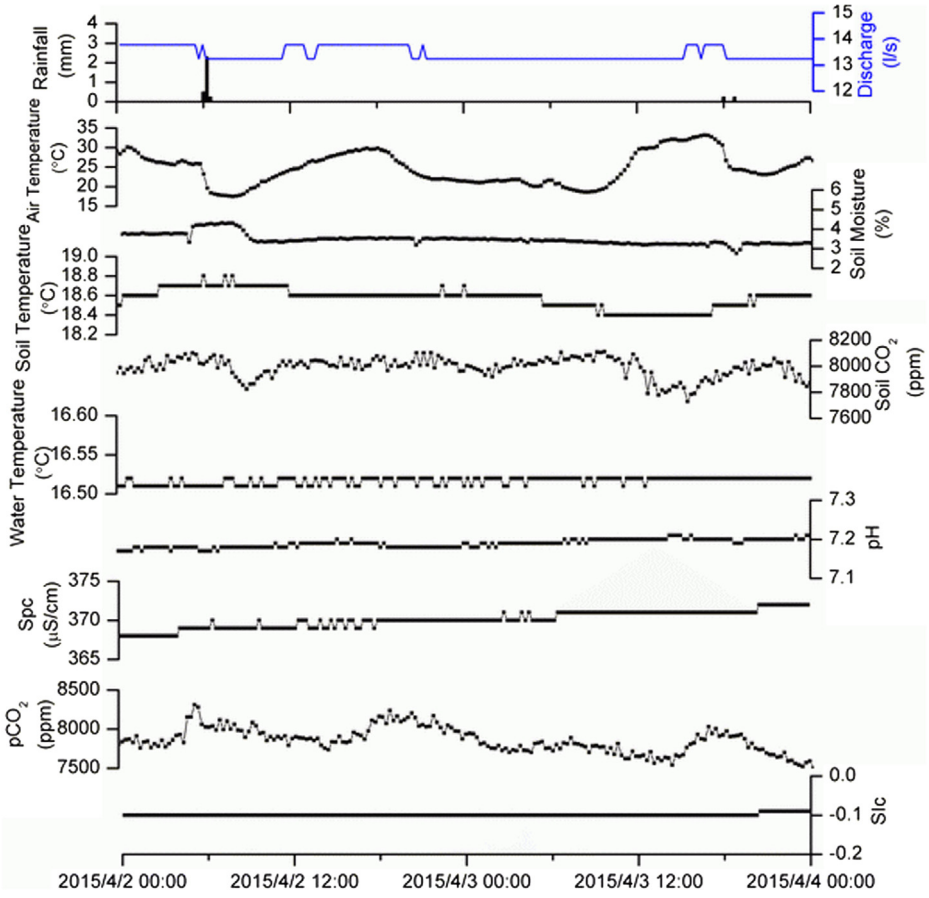


**Fig. 7.** Variations of XUR hydrochemistry and environmental parameters during a light-rain event from 2th to 4th April 2015

interaction equation (Liu et al., 2010):

$$DICf = 1/2 \sum_{t_2}^{t_1} \frac{Q_t}{A} \times 12 \times [DIC] = \frac{6}{A} \sum_{t_2}^{t_1} Q_t \times [DIC]$$

where Q is discharge in $m^3\ s^{-1}$; The factor 1/2 results from the fact that, in the case of carbonate dissolution, only half of the [DIC] is of atmospheric origin. [DIC] is concentration of DIC in mmol $L^{-1}$, DIC consists of carbonic acid, bicarbonate, and carbonate ions. In karst water, with high pH values, DIC exists as bicarbonate ions, the species of carbonic acid and carbonate ions can be neglected; A is catchment area in $m^2$; 12 is molecular weight of C.

After obtaining the discharge and [DIC] data at the outlet of the XUR in 2009–2015, the carbon sink flux per 15 min interval can be calculated by the above method. According to calculations, the average carbon sink flux at the outlet of the XUR in 2009–2015 is 1.81 g/s, 4.32 $t{\cdot}C{\cdot}a^{-1}{\cdot}km^{-2}$. The highest value appeared in 2015, up to 5.64 $t{\cdot}C{\cdot}a^{-1}{\cdot}km^{-2}$, the minimum appeared in 2010, only 3.46 $t{\cdot}C{\cdot}a^{-1}{\cdot}km^{-2}$.

## 5. Discussions

### 5.1. Factors controlling XUR $pCO_2$ variations at different time scales

In Table 5 it has been shown the controlling factors of XUR $pCO_2$ variations through PCA analysis on different scales. On a diurnal scale, PCA of the remaining variables showed that 78.2% of the variance was explained by principal component PC1 (39.1%), PC2 (21.6%) and PC3 (17.5%). Not surprisingly, soil temperature, soil moisture, soil $CO_2$ and Spc, pH had strong loadings on PC1, air temperature and discharge on PC2, indicating that soil parameters are the main factors for the diurnal variations. It can be inferred that XUR $pCO_2$ variations responded fast to variations in overlying soils. The second factor is related to discharge and air temperature, still the external parameters. On a seasonal scale, pH, Spc, $pCO_2$ and SIc had strong loadings on PC1 (30.8%), air temperature, soil temperature and discharge had strong loadings on PC2 (25.3%), water temperature and rainfall were loading on PC3 (18.0%) and PC4 (10.0%), respectively. As the first factor, pH and Spc, SIc were likely to be controlled by dissolution of carbonate rocks. The following factors revealed that temperature rather than precipitation exerted impact on $pCO_2$. Whereas on a storm scale, soil $CO_2$, water temperature, pH and SIc had a large loading on PC1 (27.6%), soil temperature and soil moisture had the strong loading on PC2 (25.4%), discharge and Spc had the loading of 23.8% on PC3. The loadings on three factors are very similar. Here, the variations from the overlying soils and climatic changes and the influence of water–rock reaction transferred very quickly to the underground system. However, the relationship between discharge and $pCO_2$ was more significant than others. It indicates that a majority of high-flow water moved inside, displaying a significant contribution on degassing conditions. Therefore, PCA analyses revealed different drivers for variations in soil $CO_2$ and $pCO_2$ at different temporal scales (Table 5). Soil components are not the only factor to influence $pCO_2$ of stream water. However, $pCO_2$ in the shallow karst water reflected the production zone of $CO_2$. Air temperature and soil temperature, reflecting daily and seasonal patterns were positively correlated with soil and stream $pCO_2$, whereas precipitation and related soil moisture were dominant during the rainfall events. The results of PCA were also discussed through the following parts.

#### 5.1.1. Factors controlling XUR $pCO_2$ variations from daily to annual scale

This study showed that the $pCO_2$ in XUR was sensitive and mainly related to soil $CO_2$ concentrations which are highly related to soil temperature and moisture (Hassan et al., 2014). Based on the daily and

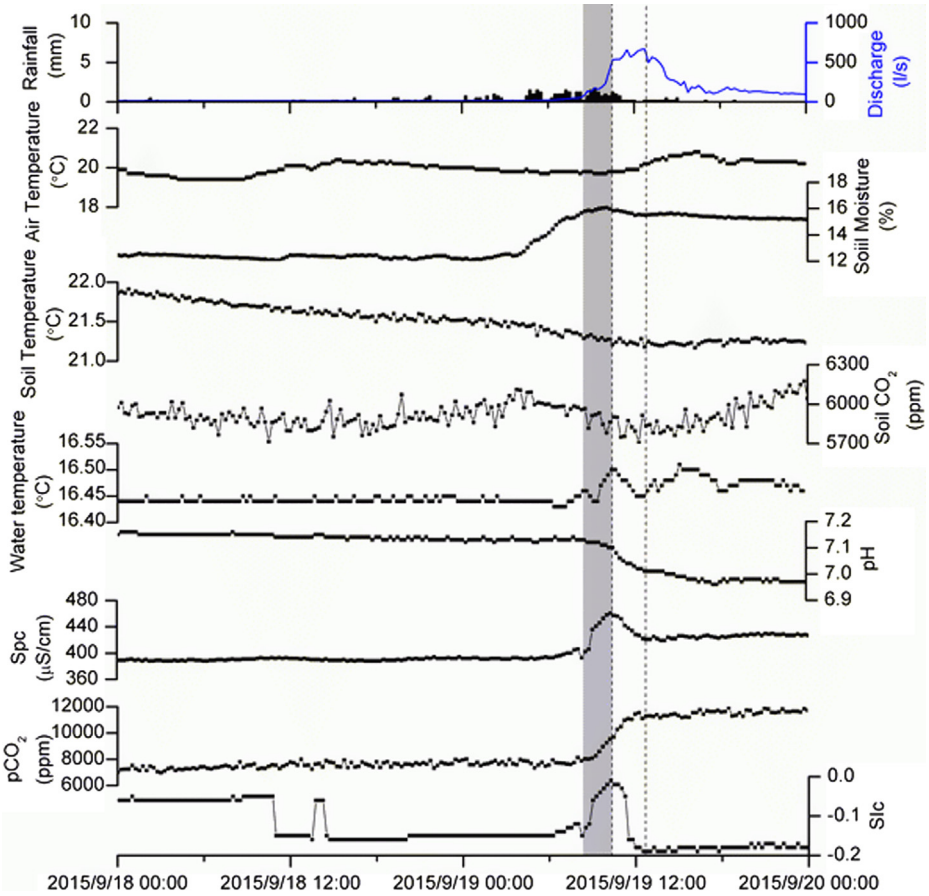


**Fig. 8.** Variations of the XUR hydrochemistry and environmental variables during a moderate-rain from 18th to 19th September 2015.

seasonal patterns of soil $CO_2$ and stream $pCO_2$, the abundant soil $CO_2$ concentration would be sufficient to sustain the cave stream $pCO_2$ (Figs. 4–6). Soil $CO_2$ mainly comes from root respiration and microbial respiration as well as decomposition of organic matter (Fairchild and Baker, 2012; Mattey et al., 2016). The variations of soil $CO_2$ concentrations lagged behind the variations of air temperature by about 6 or 8 h in spring and summer, but by 18 h in autumn and nearly no visible changes in winter (Fig. 5). Specifically, the soil $CO_2$ in spring and summer peaked at night between 22:00–24:00, which are different from those peaking at 6:00–12:00 in autumn–winter days. In spring and summer, the growing season, plants in the soil sampling plot flourished and covered the land surface, blocking solar radiation and regulating the heat conduction between the atmosphere and soil, thus delaying soil warming during daytime; while in autumn–winter season, most weeds withered to death and the soil could be heated directly by solar radiation with little vegetation cover, resulting in no or a short time lag after the variations of the soil and air temperature (Cellier et al., 1996; Yang et al., 2012). This phenomenon was also observed in Wantian Spring, SW China where the soil $CO_2$ peaked at 24:00 in spring-summer growing season but at 14:00 in autumn-winter days (Yang et al., 2012). Besides, plant respiration becomes strong at high temperatures due to the effect of photosynthesis, resulting in higher soil $CO_2$ concentrations (Atkin et al., 2000; Curiel-Yuste et al., 2007). The contribution of root respiration to the total soil $CO_2$ was greater in spring to early summer than late summer to autumn due to the seasonal distribution of root biomass (Lee et al., 2005). The direction of heat transport is opposite in daytime to that at nighttime, which can influence the velocities of $CO_2$ diffusion along soil profiles when soil warms and cools (Phillips et al., 2011). Besides, even if the reaction of $CO_2$ with the moisture or dew in alkaline soils are negligible, the significant dew deposition might exert a potential $CO_2$ sink, which partly explain that apparent $CO_2$ absorption frequently occurs at night time (Xie et al., 2009; Yates et al., 2013).

Moderate soil moisture could help to enhance the soil $CO_2$ concentrations (too low/high soil moisture will limit soil respiration) (Davidson et al., 1998; Kishimoto-Mo et al., 2015), it is important to notice that diffusion is much faster in the gas phase and the diffusive transport is determined by soil structure, porosity and soil water content (SWC) that influences water-filled pore space (Van Diest and Kesselmeier, 2008; Chen and Wang, 2014). Studies on the dependence of soil thermal parameters on soil moisture have also been reported for different kinds of soils over the years (Anandakumar et al., 2001; Wang and Shen, 2013), e.g. soil thermal conductivity is reported to increase with increased soil moisture and the dependence could be linear or nonlinear (Wang et al., 2005; Liu et al., 2008). Soil moisture had a large influence on the changes of soil microbial communities. e.g. soil moisture changed the soil particle size that was correlated with microbial diversity (Kent and Triplett, 2002) and influenced gas diffusion, $O_2$ availability and supply for microbial processes in the soil profile (Wolf et al., 2011). A significant drought (less soil moisture) occurred in the summer of 2013 due to the control of persistent subtropical high-pressure belt, resulting in a rapid decline in soil $CO_2$ concentrations, suggesting that there was an inhibitory effect of very low soil moisture on soil $CO_2$ concentrations. The correlation between soil $CO_2$ efflux and soil rewetting could be explained by the enhancement of microbial metabolism because of the availability of accumulated substrate during soil drying periods (Kim et al., 2012).

Changes in soil diffusivity regulated $CO_2$ transport rates and the availability of oxygen to aerobic soil microorganisms. Thus, soil moisture could impact the transport and storage of soil $CO_2$ in and from the soil profile on a seasonal scale (Washington et al., 1994). A significant correlation was observed between soil temperature and soil $CO_2$ in summer ($R^2 = 0.57$, $p < 0.01$), agreeing with previous studies

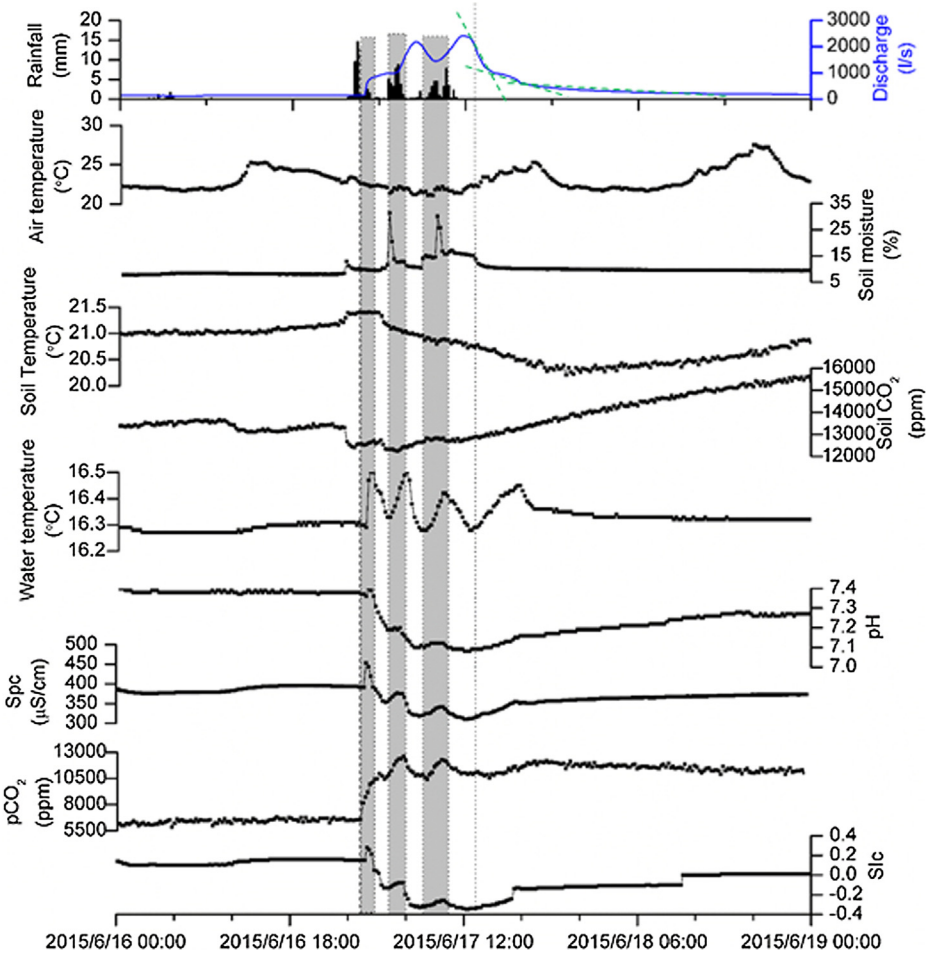


**Fig. 9.** Variations of the XUR hydrochemistry and environmental variables during a rainstorm event from 16th to 17th June 2015

**Table 5**
The results of principal component analysis on different scales.

| | Rotated component matrix on a daily scale | | | Rotated component matrix on a seasonal scale | | | | Rotated component matrix on a storm scale | | |
|---|---|---|---|---|---|---|---|---|---|---|
| | PC1 | PC2 | PC3 | PC1 | PC2 | PC3 | PC4 | PC1 | PC2 | PC3 |
| Air Temp | −0.131 | 0.880 | −0.088 | 0.119 | 0.894 | 0.120 | −0.107 | 0.227 | −0.709 | 0.071 |
| Rainfall | – | – | – | −0.019 | 0.098 | 0.029 | 0.989 | 0.081 | 0.254 | 0.189 |
| Discharge | −0.039 | 0.816 | 0.272 | 0.193 | 0.761 | 0.018 | 0.065 | 0.093 | 0.184 | 0.854 |
| Soil Temp | 0.931 | −0.099 | 0.226 | 0.226 | 0.877 | 0.120 | .-0.064 | 0.232 | 0.925 | 0.020 |
| Soil $CO_2$ | −0.620 | 0.331 | 0.561 | −0.556 | 0.412 | 0.201 | 0.033 | 0.851 | −0.107 | 0.446 |
| Water Temp | −0.041 | −0.205 | −0.758 | 0.622 | −0.094 | 0.719 | −0.018 | −0.858 | −0.363 | −0.250 |
| pH | −0.764 | 0.473 | −0.246 | 0.966 | 0.045 | −0.200 | 0.013 | 0.899 | −0.248 | −0.314 |
| Spc | 0.958 | 0.043 | −0.067 | −0.707 | 0.346 | −0.522 | −0.049 | −0.230 | 0.530 | −0.664 |
| $pCO_2$ | 0.684 | −0.293 | 0.109 | −0.893 | 0.152 | 0.212 | −0.107 | −0.144 | 0.187 | 0.769 |
| SIc | 0.366 | −0.403 | 0.642 | 0.864 | 0.203 | −0.425 | 0.008 | 0.755 | −0.011 | −0.603 |
| Soil Moisture | −0.734 | −0.297 | 0.486 | – | – | – | – | −0.094 | 0.909 | 0.306 |
| Variance (%) | 39.1 | 21.6 | 17.5 | 30.8 | 25.3 | 18.0 | 10.1 | 27.6 | 25.4 | 23.8 |

*Extact method: Principal component analysis, PC1-PC4 stands for principal components.

that soil $CO_2$ was mainly controlled by soil temperature (Hashimoto et al., 2009; Kishimoto-Mo et al., 2015). Transpiration, a vital component in soil-water-plant relationship is of particular importance in studying possible interactions of elevated $CO_2$ and water supply in terms of plant water use (Madhu and Hatfield, 2014). Low soil moisture and high permeability would likely exaggerate advective transport of $CO_2$ across the soil surface. Rates of soil respiration increased from winter to summer could be due to the increased temperature and precipitation in a monsoon climatic region, which explained the more abundant $CO_2$ in the summer of 2015 than that of 2013 when the precipitation was less than normal years. Higher soil $CO_2$ concentration occurred in warm and wet summer under the effects of soil temperature and soil moisture. Besides, increasing air temperature could stimulate organic matter decomposition in the soil (Davidson and Janssens, 2006), and then produce more soil $CO_2$.

The daily variations of $pCO_2$ in XUR co-varied with soil $CO_2$ concentrations in the same amplitude though the variations of $pCO_2$ lagged behind the changes of soil $CO_2$ concentrations by a few hours in different seasons (Fig. 5). $pCO_2$ (higher in autumn and lower in winter) also showed consistent changes with Spc ($R^2 = 0.66$, $p < 0.01$, $n = 28$) on a seasonal scale, and there was also positive correlation between pH and SIc ($> 0$) on a seasonal scale ($R^2 = 0.88$, $p < 0.01$,

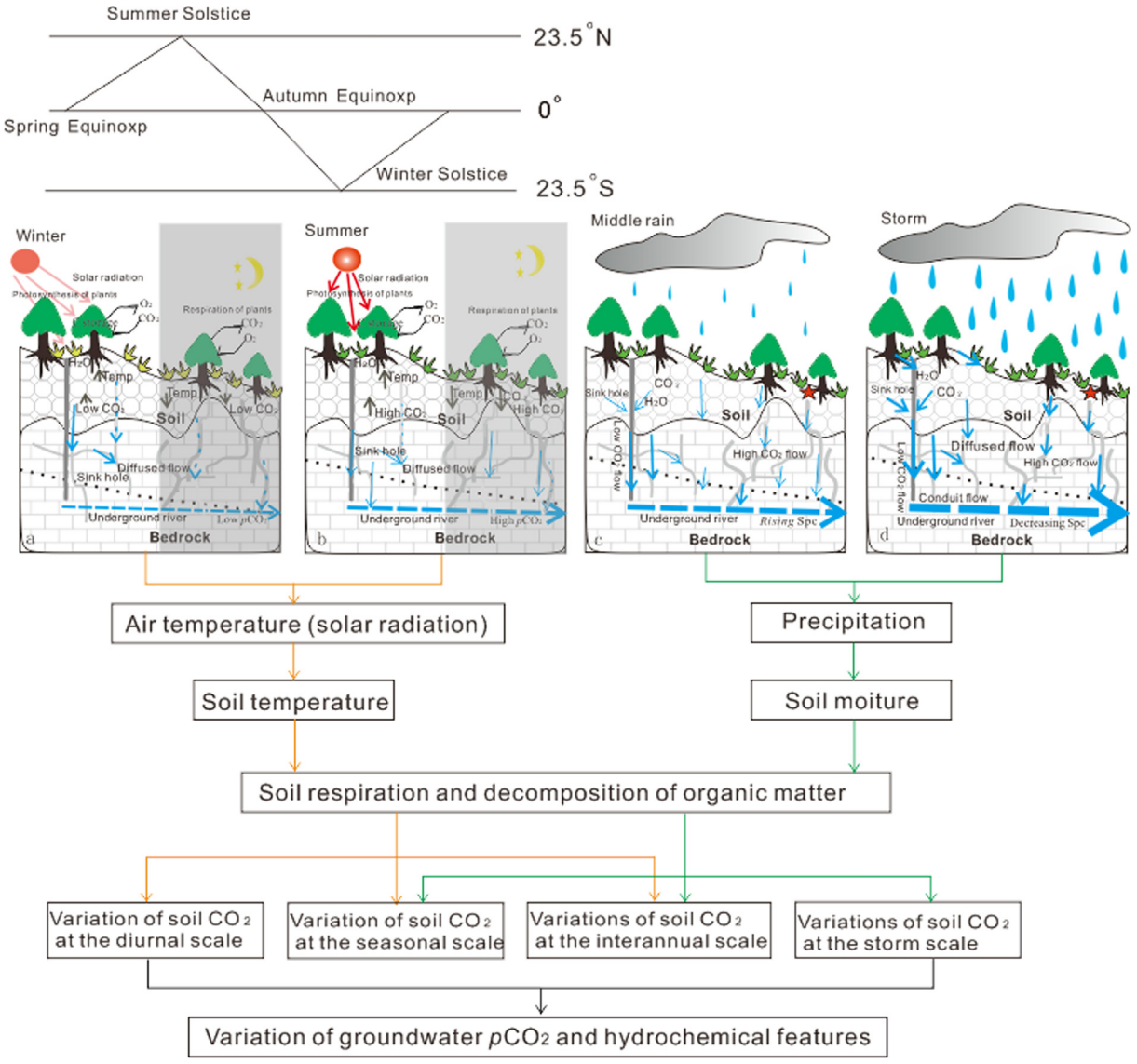


**Fig. 10.** Diagram illustrating the pathways between $CO_2$ reservoirs and movement from soil to karst underground river dominated by main factors at different scales.

n = 28). Daily and seasonal trends in stream $pCO_2$ were lagged behind the trends in soil $CO_2$. The consistent pattern of daily variations in soil $CO_2$ and stream $pCO_2$ indicated the fast response of stream water to climatic change (e.g. temperature), whereas the seasonal patterns of soil $CO_2$ and stream $pCO_2$ suggested that the cave system buffers the environmental fluctuation (Fig. 6).

1634490371475The consistently varied stream $pCO_2$ values suggest that soil $CO_2$ was one of the C sources to the stream (Liu et al., 2007), as the following equation expresses:

Variations of soil $CO_2$ caused the fluctuation of stream $pCO_2$ (Liu et al., 2007), resulting in variations in pH, Spc and SIc. Thus, higher soil $CO_2$ concentration in spring-summer seasons were always related to higher stream $pCO_2$, but lower pH, Spc and SIc.

From 2009 to 2015, air temperature and precipitation overall had an upward trend in the study area, the XUR water $pCO_2$ also showed an upward trend (Table 4). The increase of air temperature could lead to an increase in soil $CO_2$ concentrations and stream $pCO_2$. Precipitation has increased especially during 2014–2015 due to the El Niño phenomenon. Interannual variations in precipitation were more distinct than variations in temperature, confirming that the soil moisture is substantial over an annual scale (Pla et al., 2016). We have no continuous monitoring data of soil moisture for all these 7 years. However, the increasing precipitation and discharge indicate that annual soil moisture would be elevated during this period. More precipitation and increased discharge resulted in declines of Spc, pH and SIc as “dilution effect”. This phenomenon on an annual scale can be considered as amplified “dilution effect” of rainfall events. Gassing and degassing are rapid processes compared to dissolution and precipitation in non-turbulent flow (Ford and Willams, 2007). The increase in $pCO_2$ and the decrease in SIc and pH suggested important effects of climate change on the dissolution of limestone in the study area even though the water temperature only slightly changed.

### 5.1.2. *Factors controlling XUR $pCO_2$ variations on a storm scale*

Rainwater could dissolve soil $CO_2$ and infiltrate into the underground system, resulting in high $pCO_2$, low pH in the underground river due to water-rock interaction process (Liu et al., 2007). Soil moisture, soil $CO_2$ concentrations and discharge resulted from the increased precipitation are primary controlling factors for the $pCO_2$ variations in the XUR on a storm scale, which is actually related to water-carbonate rock reaction. During rainfall events, water rapidly poured into the system via sinkholes and vertical drains, infiltration reached the XUR within several hours due to a storm input. The light rain did not exert special effects on the hydrochemical variations in the XUR, only $pCO_2$

changed in line with soil $CO_2$. The XUR $pCO_2$ made a fast response to the infiltrated soil $CO_2$ in 3–6 h (Fig. 7). This phenomenon could be explained that soil $CO_2$ was dissolved in rainwater and went into the XUR, resulting in reduced soil $CO_2$ concentration in the soil spaces. Continuously, when the infiltrated water with high $CO_2$ concentration entered the underground system, the XUR $pCO_2$ could be increased along with the increased discharge. During a moderate rainfall process (Fig. 8), soil $CO_2$ concentrations decreased as the rainwater dissolved soil $CO_2$ and infiltrated into the XUR to increase $pCO_2$. Moreover, excessive soil moisture affected the exchange of soil $CO_2$ and outside oxygen, inhibiting soil autotrophic respiration and heterotrophic respiration (Cook and Orchard, 2008). Rainwater which had infiltrated into the groundwater resulted in a "$CO_2$ effect" that is characterized by increasing discharge, Spc, $pCO_2$, SIc and water temperature in the underground river (Liu et al., 2007). With the rainfall continues, rainfall intensity exceeded the infiltration rate of the surface soil, and rainwater began to form part of overland flow and drained through larger pipelines, resulting in "dilution effect" with decreasing Spc, pH and SIc in XUR. More complicated processes in hydrograph and chemograph were observed during the storm (Fig. 9).

It was obvious that soil $CO_2$ concentration was decreasing at the beginning of rainfall events. However, the decreasing magnitude and responding time seemed to be related to the intensities of the rainfall events. For example, the soil $CO_2$ concentration went down sharply and quickly during the first phase of the storm with a high rainfall intensity compared to the third one with a low rainfall intensity. All the hydrochemical parameters in the XUR, such as water temperature, Spc, $pCO_2$ and SIc responded quickly to the storm, indicating the existence of sinkholes, large conduits that allowed the rainwater to go quickly through the surface to the underground system (Fig. 1). The changes of these parameters at different stages of storms revealed different processes that controlled the hydrochemical features. The monitored parameters made a quick response (within 5 h) to the rainfall events, agreeing with that there are sinkholes that allow the rainwater to go quickly to underground system (Fig. 10). However, the high $pCO_2$ values in XUR water indicated the dissolution of soil $CO_2$ during the rainfall processes. Kovács and Perrochet (2008) showed that hydrographs of homogeneous flow domains can be decomposed into an infinite number of exponential components and that only three of these components contribute significantly to total discharge. In our study, the XUR hydrograph can be decomposed into three segments during a storm (Fig. 9). Discharge and intrinsic drivers are important factors for the $pCO_2$ variations in XUR. Investigating the hydrodynamic functioning during a recharge event allows us to understand the flow mechanisms taking place between the matrix and fracture systems in the karst aquifer.

In a subtropical region, the rainwater infiltrating into the ground system in summer holds higher temperature than the cave stream water. This phenomenon was also observed in other subtropical springs, such as Maolan Spring (Liu et al., 2007). The three peaks of XUR temperatures during the storm indicated the inputs of fresh recharge, accompanying with increased $pCO_2$ and Spc (Fig. 9). The increased $pCO_2$ values in phase might be attributed to the rapid recharge and the elevated $CO_2$ values resulted from some interaction with the soil/residuum zone and finally went along with the conduit flow. Ecosystem respiration is expected to increase as the soils become rehydrated (Barr et al., 2007), which could explain the increased soil $CO_2$ after rainfall events or rainy season.

In general, the "$CO_2$ effect" and "dilution effect" were alternately dominant and the $pCO_2$ variations in XUR, Spc, pH and SIc fluctuated largely at different stages of rainfalls. In this study, the occurrence of "$CO_2$ effect" and "dilution effect" were highly related to rainfall intensities. The $pCO_2$ changes lagging behind the soil moisture changes during a moderate rain that masked the effects of soil $CO_2$, result in delayed $pCO_2$ changes in comparison with Spc and SIc that might be controlled by the dissolution of carbonate rocks before the main recharge or the thick residuum in the spring (Vesper and White, 2004). The Spc corresponding in phase with SIc indicated that the most aggressive water signified by the lowest SIc values occurred during the main storm process. XUR hydrochemistry changes were mainly dominated by precipitation (soil moisture) and soil $CO_2$ that were as driving factors during storms. During the light rain, $pCO_2$ showed in-phase change with soil $CO_2$, indicating significant $CO_2$ effects from the soils. However, the specific variational processes between soil $CO_2$ and XUR $pCO_2$ might change due to soil moisture that dissolves soil $CO_2$ and finally exerts impact on XUR $pCO_2$.

### 5.2. Relationship of soil $CO_2$-XUR $pCO_2$ and the cave carbon sink/source

This soil $CO_2$-stream $CO_2$ interaction reveals the complex processes in the karst area. The air temperature and soil $CO_2$ concentrations showed a good agreement and consistency on diel and seasonal scales. The significant seasonal variation of soil $CO_2$ flux was found during late spring and early summer as a result of optimal environmental conditions and spring growth flush (Baldocchi et al., 1981). Seasonal variability of soil $CO_2$ was mainly controlled by soil temperature, leading to seasonal variations in XUR water $pCO_2$. Interannual variability of soil $CO_2$ was greatly affected by changes in soil water content that is one of indirect abiotic factors for soil $CO_2$ production and transport (Griffis et al., 2004; Hassan et al., 2014). The generated soil $CO_2$ could diffuse quickly into the XUR system via karst fissures and conduits in the karstified limestone (Fig. 10). The $pCO_2$ was increased, following the increased precipitation and soil $CO_2$ concentrations as well as the current air temperature that increased slightly from 2009 to 2015. In addition, higher XUR $pCO_2$ in summer and autumn could also be affected by different transport patterns that are controlled by complicated conduit systems and soil moisture (Birk et al., 2004). The DIC flux has been increasing in the last 7 years, which should be taken attention in the calculation of carbon cycle. The long-term increase in $pCO_2$ of XUR greater than the increase of atmospheric $CO_2$. We found that the calculated quantity of carbon sink increased by up to 38% over the 7 years, indicating clearly that karst ground cave stream is a $CO_2$ sink through the dissolution of limestones.

## 6. Conclusions

The results based on seven-year continuous monitoring show that Xueyu Cave watershed is a dynamic and varied system in terms of hydrochemistry. Interannual, seasonal, daily and storm-scale variations were continuously observed for pH, Spc, $pCO_2$ and SIc in the cave stream. The variability of these hydrochemical features tended to be in the order of storm-scale > seasonal > interannual > daily scale.

The seasonal and daily variations of these features varied with soil temperature which influenced soil $CO_2$ concentration that was always the primary driving force for the variations of XUR $pCO_2$. The relationship between soil $CO_2$ and XUR $pCO_2$ on daily and seasonal scales indicates the fast response of stream $pCO_2$ to the overlying soil.

The storm-scale fluctuations of soil $CO_2$ concentrations occurred during the spring-summer rainy days, mainly controlled by soil moisture, and the rainfall intensity. The interannual-scale changes are mainly under the influences of precipitation and temperature, so the increasing annual average temperature and precipitation resulted in elevated soil $CO_2$ and XUR $pCO_2$.

The calculation of carbon flux using DIC ($HCO_3^-$) shows that the carbon sink flux from 2009 to 2015 had been increasing, from 3.46 to 5.64 t $C{\cdot}a^{-1}{\cdot}km^{-2}$ with the mean value of 4.32 t $C{\cdot}a^{-1}{\cdot}km^{-2}$. The carbon sink in the karst groundwater increased by 38% over the 7 year.

The study on high-resolution continuous monitoring in surface-subterranean from local scales to broader scales requires further investigation on the potential impact of soil $CO_2$-$pCO_2$ changes, which can provide much more valuable information on the system behaviour in future carbon cycle studies. Our study put a flash light on the fact

that soil $CO_2$ has a significant tendency to convert C to the underground river in a quick flow which may play an important role in the studies of global warming.

## Acknowledgements

This research was financed by the National Key Research and Developmental program of China (2016YFC0502306), the National Natural Science Foundation of China (NSF Grant no. 41472321) and the open project from Chongqing Key Laboratory of Karst Environment (Cqk201701). Thanks to Ze Zeng, XianFu Lv, Jiaqi Lei, Ge Hu and Sibo Zeng who helped with the field work. Thanks to all other students who made contributions to the cave monitoring.

## References

Anandakumar, K., Venkatesan, R., Prabha, T.V., 2001. Soil thermal properties at kalpakkam in coastal south India. J. Earth Syst. Sci. 110 (3), 239–245. https://doi.org/10.1007/BF02702239.

Atkin, O.K., Edwards, E.J., Loveys, B.R., 2000. Response of root respiration to changes in temperature and its relevance to global warming. New Phytol. 147 (1), 141–154. https://doi.org/10.1046/j.1469-8137.2000.00683.x.

Baldini, J.U.L., McDermott, F., Hoffmann, D.L., Richards, D.A., Clipson, N., 2008. Very high-frequency and seasonal cave atmosphere $pCO_2$ variability: implications for stalagmite growth and oxygen isotope-based paleoclimate records. Earth Planet. Sci. Lett. 272, 118–129. https://doi.org/10.1016/j.epsl.2008.04.031.

Baldocchi, D., Verma, S., Rosenberg, N., 1981. Seasonal and diurnal variation in the $CO_2$ flux and $CO_2$—water flux ratio of alfalfa. Agri. Meteor. 23 (3), 231–244. https://doi.org/10.1016/0002-1571(81)90107-2.

Barr, A.G., Black, T.A., Hogg, E.H., Griffis, T.J., Morgenstern, K., Kljun, N., Theede, A., Nesic, Z., 2007. Climatic controls on the carbon and water balances of a boreal aspen forest, 1994–2003. Global Change Biol. 13 (3), 561–576. https://doi.org/10.1111/j.1365-2486.2006.01220.x.

Berner, R.A., 2003. The long-term carbon cycle, fossil fuels and atmospheric composition. Nature 426, 323–326.

Birk, S., Liedl, R., Sauter, M., 2004. Identification of localised recharge and conduit flow by combined analysis of hydraulic and physico-chemical spring responses (Urenbrunnen, SW-Germany). J. Hydrol. 286 (1), 179–193. https://doi.org/10.1016/j.jhydrol.2003.09.007.

Cellier, P., Richard, G., Robin, P., 1996. Partition of sensible heat fluxes into bare soil and the atmosphere. Agric. For. Meteorol. 82 (1–4), 245–265. https://doi.org/10.1016/0168-1923(95)02328-3.

Chen, X., Wang, W.F., 2014. On the apparent $CO_2$ absorption by alkaline soils. Biogeosci. Discuss. 11 (2), 2665–2683. https://doi.org/10.5194/bgd-11-2665-2014.

Cholet, C., Charlier, J.B., Moussa, R., Steinmann, M., Denimal, S., 2017. Assessing lateral flows and solute transport during floods in a conduit-flow-dominated karst system using the inverse problem for the advection–diffusion equation. Hydrol. Earth Syst. Sci. 21, 3635–3653. https://doi.org/10.5194/hess-21-3635-2017.

Cook, F.J., Orchard, V.A., 2008. Relationships between soil respiration and soil moisture. Soil Biol. Biochem. 5, 1013–1018.

Cuezva, S., Fernandez-Cortes, A., Benavente, D., Serrano-Ortiz, P., Kowalski, A.S., Sanchez-Moral, S., 2011. Short-term $CO_2$(g) exchange between a shallow karstic cavity and the external atmosphere during summer: role of the surface soil layer. Atmos. Environ. 45 (7), 1418–1427. https://doi.org/10.1016/j.atmosenv.2010.12.023.

Curiel-Yuste, J., Baldocchi, D.D., Gershenson, A., Goldstein, A., Misson, L., Wong, S., 2007. Microbial soil respiration and its dependency on carbon inputs, soil temperature and moisture. Glob. Change Biol. 13, 1–18. https://doi.org/10.1111/j.1365-2486.2007.01415.x.

Davidson, E.A., Elizabeth, B., Boone, R.D., 1998. Soil water content and temperature as independent or confounded factors controlling soil respiration in a temperate mixed hardwood forest. Glob. Change Biol. 4 (4), 412–418. https://doi.org/10.1046/j.1365-2486.1998.00128.x.

Davidson, E.A., Janssens, I.A., 2006. Temperature sensitivity of soil carbon decomposition and feedbacks to climate change. Nature 440 (7081), 165–173. https://doi.org/10.1038/nature04514.

de Montety, V., Martin, J.B., Cohen, M.J., Foster, C., Kurz, M.J., 2011. Influence of diel biogeochemical cycles on carbonate equilibrium in a karst river. Chem. Geol. 283 (1–2), 31–43. https://doi.org/10.1016/j.chemgeo.2010.12.025.

Dreybrodt, W., 1988. Chemistry of the system H2O-CO2-CaCO3. Processes in Karst Systems: Physics, Chemistry and Geology. Springer Berlin Heidelberg., vol. 4, pp. 13–42, ISBN 978-3-642-83352-6.

Faimon, J., Troppová, D., Baldík, V., Novotny, R., 2012. Air circulation and its impact on microclimatic variables in the Císařská Cave (Moravian Karst, Czech Republic). Int. J. Climatol. 32 (4), 599–623.

Fairchild, I.J., Baker, A., 2012. Speleothem Science. From Process to Past Environment. Wiley-Blackwell, Oxford. pp. 450, ISBN: 978-1-405-19620-8.

Fernandez-Cortes, A., Sanchez-Moral, S., Cuezva, S., Benavente, D., Abella, R., 2011. Characterization of trace gases' fluctuations on a 'low energy' cave (Castañar de Ibor, Spain) using techniques of entropy of curves. Int. J. Climatol. 31 (1), 127–143. https://doi.org/10.1002/joc.2057.

Frisia, S., Fairchild, I.J., Fohlmeister, J., Miorandi, R., Spötl, C., Borsato, A., 2011. Carbon mass-balance modelling and carbon isotope exchange processes in dynamic caves. Geochim. Cosmochim. Acta 75 (2), 380–400.

Ford, D.C., Willams, P.W., 2007. Karst Hydrogeology and Geomorphology. Wiley, Chichester, UK. pp. 562, ISBN: 9780470849972.

Griffis, T.J., Black, T.A., Gaumont-Guay, D., Drewitt, G.B., Nesic, Z., Barr, A.G., Morgenstern, K., Kljun, N., 2004. Seasonal variation and partitioning of ecosystem respiration in a southern boreal aspen forest. Agri. Fore. Meteor. 125 (3–4), 207–223. https://doi.org/10.1016/j.agrformet.2004.04.006.

Gulley, J.D., Martin, J.B., Moore, P.J., Murphy, J., 2013. Formation of phreatic caves in an eogenetic karst aquifer by $CO_2$ enrichment at lower water tables and subsequent flooding by sea level rise. Earth Surf. Proc. Land. 38, 1210–1224. https://doi.org/10.1002/esp.3358.

Hartmann, A., Goldscheider, N., Wagener, T., Lange, J., Weiler, M., 2014. Karst water resources in a changing world: Review of hydrological modeling approaches. Rev. Geophys. 52, 1–25. https://doi.org/10.1002/2013RG000443.

Hashimoto, T., Miura, S., Ishizuka, S., 2009. Temperature controls temporal variation in soil $CO_2$ efflux in a secondary beech forest in Appi Highlands, Japan. J. For. Res. 14, 44–50. https://doi.org/10.1007/s10310-008-0096-2.

Hassan, W., David, J., Abbas, F., 2014. Effect of type and quality of two contrasting plant residues on $CO_2$, emission potential of ultisol soil: implications for indirect influence of temperature and moisture. Catena 114 (5), 90–96. https://doi.org/10.1016/j.catena.2013.11.001.

Hess, J.W., White, W.B., 1988. Storm response of the karstic carbonate aquifer of south central Kentuck. J. Hydrol. 99, 235–252. https://doi.org/10.1016/0022-1694(88)90051-0.

Huang, S., Qing, H., Huang, P., Hu, Z., Wang, Q., Zou, M., Liu, H., 2008. Evolution of strontium isotopic composition of seawater from Late Permian to Early Triassic based on study of marine carbonates, Zhongliang Mountain, Chongqing, China. Sci. China Ser. D Earth Sci. 51 (4), 528–539. https://doi.org/10.1007/s11430-008-0034-3.

IPCC, Summary for policymakers. In: Climate Change 2013: The Physical Science Basis. Contribution of Working Group I to the Fifth Assessment Report of the Intergovernmental Panel on Climate Change (eds Stocker, T.F., Qin, D., Plattner, G.-K., Tignor, M., Allen, S.K., Boschung, J., Nauels, A., Xia, Y., Bex, V., Midgley, P.M.), Cambridge University Press, Cambridge, UK and New York, NY, USA. pp. 3–29.

Jiang, Y., Hu, Y., Schirmer, M., 2013. Biogeochemical controls on daily cycling of hydrochemistry and $\delta^{13}C$ of dissolved inorganic carbon in a karst spring-fed pool. J. Hydrol. 478, 157–168. https://doi.org/10.1016/j.jhydrol.2012.12.001.

Kent, A.D., Triplett, E.W., 2002. Microbial communities and their interactions in soil and rhizosphere ecosystems. Annu. Rev. Microbiol. 56, 211–236. https://doi.org/10.1146/annurev.micro.56.012302.161120.

Kim, D.G., Vargas, R., Bond-Lamberty, B., Turetsky, M.R., 2012. Effects of soil rewetting and thawing on soil gas fluxes: a review of current literature and suggestions for further research. Biogeosciences 9, 2459–2483. https://doi.org/10.5194/bg-9-2459-2012.

Kishimoto-Mo, A.W., Masaki-Uchida, S.Y., Kondo, M., Hiroshi Koizumi, S.M., 2015. Contribution of soil moisture to seasonal and annual variations of soil $CO_2$ efflux in a humid cool-temperate oak-birch forest in central Japan. Ecol. Res. 30, 311–325. https://doi.org/10.1007/s11284-015-1254-6.

Kovács, A., Perrochet, P., 2008. A quantitative approach to spring hydrograph decomposition. J. Hydrol. 352, 16–29. https://doi.org/10.1016/j.jhydrol.2007.12.009.

Kowalczk, A.J., Froelich, P.N., 2010. Cave air ventilation and $CO_2$ outgassing by radon-222 modeling: how fast do cave breathe? Earth Planet Sci. Lett. 289, 209–219. https://doi.org/10.1016/j.epsl.2009.11.010.

Lee, M.S., Nakane, K., Nakatsubo, T., Koizumi, H., 2005. The importance of root respiration in annual soil carbon fluxes in a cool-temperate deciduous forest. Agr. Forest Meteorol. 134, 95–101. https://doi.org/10.1016/j.agrformet.2005.08.011.

Li, J.H., Qi, Y.Q., Zhong, Y., Yang, L.H., Xu, Y.Q., Lin, P., Wang, S.F., He, J., 2016. Karst aquifer characterization using storm event analysis for Black Dragon springshed, Beijing, China. Catena 145, 30–38. https://doi.org/10.1016/j.catena.2016.05.019.

Liu, H., Wang, B., Fu, C.B., 2008. Relationships between surface albedo, soil thermal parameters and soil moisture in the semi-arid area of Tongyu, northeastern China. Adv. in Atmos. Sci. 25 (5), 757–776 in Chinese with English abstract.

Liu, Z., Zhao, J., 2000. Contribution of carbonate rock weathering to the atmospheric $CO_2$ sink. Environ. Geol. 39 (9), 1053–1058.

Liu, Z., Li, Q., Sun, H., Wang, J., 2007. Seasonal, diurnal and storm-scale hydrochemical variations of typical epikarst springs in subtropical karst areas of SW China: soil $CO_2$ and dilution effects. J. Hydrol. 337 (1–2), 207–223. https://doi.org/10.1016/j.jhydrol.2007.01.034.

Liu, Z., Dreybrodt, W., Wang, H., 2010. A new direction in effective accounting for the atmospheric $CO_2$ budget: considering the combined action of carbonate dissolution, the global water cycle and photosynthetic uptake of DIC by aquatic organisms. Earth Sci. Rev. 99 (3–4), 162–172. https://doi.org/10.1016/j.earscirev.2010.03.001.

Madhu, M., Hatfield, J.L., 2014. Interaction of carbon dioxide enrichment and soil moisture on photosynthesis, transpiration, and water use efficiency of soybean. Agr. Sci. 05 (5), 410–429 http://www.scirp.org/journal/ashttp://dx.doi.org/10.4236/as.2014.55043.

Mattey, D.P., Atkinson, T.C., Barker, J.A., Fisher, R., Latin, J.P., Durrell, R., Ainsworth, M., 2016. Carbon dioxide, ground air and carbon cycling in Gibraltar karst. Geochim. Cosmochim. Acta 184, 88–113. https://doi.org/10.1016/j.gca.2016.01.041.

Morse, J.W., Arvidson, R.S., 2002. The dissolution kinetics of major sedimentary carbonate minerals. Earth Sci. Rev. 58 (1–2), 51–84. https://doi.org/10.1016/S0012-8252(01)00083-6.

Phillips, C.L., Nickerson, N., Risk, D., Bond, B.J., 2011. Interpreting diel hysteresis between soil respiration and temperature. Global Change Biol. 17, 515–527. https://doi.org/10.1111/j.1365-2486.2010.02250.x.

Pla, C., Cuezva, S., Garcia-Anton, E., Fernandez-Cortes, A., Cañaveras, J.C., Sanchez-Moral, S., Benavente, D., 2016. Changes in the $CO_2$ dynamics in near-surface cavities under a future warming scenario: factors and evidence from the field and experimental findings. Sci. Total Environ. 565, 1151–1164. https://doi.org/10.1016/j.scitotenv.2016.05.160.

Pla, C., Cuezva, S., Martinez-Martinez, J., Fernandez-Cortes, A., Garcia-Anton, E., Fusi, N., Crosta, G.B., Cuevas-Gonzalez, J., Cañaveras, J.C., Sanchez-Moral, S., Benaventeaet, D., 2017. Role of soil pore structure in water infiltration and $CO_2$ exchange between the atmosphere and underground air in the vadose zone: a combined laboratory and field approach. Catena 149, 402–416.

Pu, J., Yuan, D., Zhao, H., Shen, L., 2014. Hydrochemical and $pCO_2$, variations of a cave stream in a subtropical karst area, Chongqing, SW China: piston effects, dilution effects, soil $CO_2$, and buffer effects. Environ. Earth Sci. 71 (9), 4039–4049. https://doi.org/10.1007/s12665-013-2787-z.

Pu, J., Wang, A., Yin, J., Shen, L., Sun, Y., Yuan, D., Zhao, H., 2015. Processes controlling dripwater hydrochemistry variations in Xueyu Cave, SW China: implications for speleothem palaeoclimate signal interpretations. Boreas 44, 603–617. https://doi.org/10.1111/bor.12117.

Pu, J., Wang, A., Shen, L., Yin, J., Yuan, D., Zhao, H., 2016. Factors controlling the growth rate, carbon and oxygen isotope variation in modern calcite precipitation in a subtropical cave, Southwest China. J. Asian Earth Sci. 119, 167–178. https://doi.org/10.1016/j.jseaes.2015.12.010.

Quinlan, J.F., Alexander, J.E.C., 1987. How often should samples be taken at relevant locations for reliable monitoring of pollutants from an agricultural, waste disposal, or spill site in a karst terrane? A first approximation, In: Beck, B.F., Wilson, W.L. (Eds.), Proceedings of Multidisciplinary Conference on Sinkholes and Environmental Impacts of Karst. A.A. Balkema, Rotterdam. pp. 277–293.

Ryan, M., Meiman, J., 1996. An examination of short-term variations in water quality at a karst spring in Kentucky. Ground Water 34, 23–30. https://doi.org/10.1111/j.1745-6584.1996.tb01861.x.

Serrano-Ortiz, P., Roland, M., Sanchez-Moral, S., Janssens, I.A., Domingo, F., Godderis, Y., Kowalski, A.S., 2010. Hidden, abiotic $CO_2$ flows and gaseous reservoirs in the terrestrial carbon cycle: review and perspectives. Agric. For. Meteorol. 150, 321–329. https://doi.org/10.1016/j.agrformet.2010.12.005.

Spötl, C., Fairchild, I.J., Tooth, A.F., 2005. Speleothem deposition in a dynamically ventilated cave, Obir Caves (Austrian Alps). Evidence from cave air and drip water monitoring. Geochim. Cosmochim. Acta 69, 2451–2468.

Stumm, W., Morgan, J.J., 1981. Aquatic Chemistry, second ed. Wiley Interscience, New York.

Van Diest, A., Kesselmeier, J., 2008. Soil atmosphere exchange of carbonyl sulfide regulated by diffusivity depending on water-filled pore space. Biogeosciences 5, 475–483. https://doi.org/10.5194/bg-5-475-2008.

Vesper, D.J., White, W.B., 2004. Storm pulse chemographs of saturation index and carbon dioxide pressure: implications for shifting recharge sources during storm events in the karst aquifer at Fort Campbell, Kentucky/Tennessee, USA. Hydrogeol. J. 12 (2), 135–143. https://doi.org/10.1007/s10040-003-0299-8.

Washington, J.W., Rose, A.W., Ciolkosz, E.J., Dobos, R.R., 1994. Gaseous diffusion and permeability in four soil profiles in central Pennsylvania. Soil Sci. 157, 65–76. https://doi.org/10.1097/00010694-199402000-00001.

Wang, K., Wang, P., Liu, J., Sparrow, M., Haginoya, S., Zhou, X., 2005. Variation of surface albedo and soil thermal parameters with soil moisture content at a semi-desert site on the western Tibetan plateau. Bound-Lay Meteorol. 116 (1), 117–129. https://doi.org/10.1007/s10546-004-7403-z.

Wang, Y., Shen, G.M., 2013. The primary and secondary analysis of uncertain factors in soil thermal properties for GSHP. Adv. Mater. Resear. 614–615, 688–694. https://doi.org/10.4028/www.scientific.net/AMR.614-615.688.

Wigley, T.M.L., 1977. WATSPEC: a computer program for determining equilibrium speciation of aqueous solutions. Br. Geomorphol. Res. Gr. Tech. Bull. 20, 1–48.

Wolf, B., Chen, W., Brüggemann, N., Zheng, X., Pumpanen, J., Butterbach-Bahl, K., 2011. Applicability of the soil gradient method for estimating soil-atmosphere $CO_2$, $CH_4$, and $N_2O$ fluxes for steppe soils in Inner Mongolia. J. Plant Nut. Soil Sci. 174, 359–372. https://doi.org/10.1002/jpln.201000150.

Wu, K., Shen, L., Zhang, T., Xiao, Q., Wang, A., 2015. Links between host rock, water, and speleothems of Xueyu Cave in Southwestern China: lithology, hydrochemistry, and carbonate geochemistry. Arab. J. Geosci. 8 (11), 8999–9013. https://doi.org/10.1007/s12517-015-1876-6.

Xie, J.X., Li, Y., Zhai, C.X., Li, C.H., Lan, Z.D., 2009. $CO_2$ absorption by alkaline soils and its implication to the global carbon cycle. Environ. Geol. 56, 953–961. https://doi.org/10.1007/s00254-008-1197-0.

Yates, E.L., Detweiler, A.M., Iraci, L.T., Bebout, B.M., McKay, C.P., Schiro, K., Sheffner, E.J., Kelley, C.A., Tadić, J.M., Loewenstein, M., 2013. Assessing the role of alkaline soils on the carbon cycle at a playa site. Environ. Earth Sci. 70, 1047–1056. https://doi.org/10.1007/s12665-012-2194-x.

Yang, R., Liu, Z., Zeng, C., Zhao, M., 2012. Response of epikarst hydrochemical changes to soil $CO_2$ and weather conditions at Chenqi, Puding, SW China. J. Hydrol. 468–469 (22), 151–158. https://doi.org/10.1016/j.jhydrol.2012.08.029.

Zhao, M., Zeng, C., Liu, Z., Wang, S., 2010. Effect of different land use/land cover on karst hydrogeochemistry: a paired catchment study of Chenqi and Dengzhanhe, Puding, Guizhou, SW China. J. Hydrol. 388 (1–2), 121–130. https://doi.org/10.1016/j.jhydrol.2010.04.034.

Zharkov, M.A., Chumakov, N.M., 2001. Paleogeography and sedimentation settings during Permian-Triassic reorganizations in biosphere. Stratigr. Geol. Correl. 9 (4), 340–363 https://doi.org/http://khramovs.nm.ru/biblio/geo/chumakov-2001.pdf.

Zhu, X., Zhang, Y., Han, D., Wei, R., Chen, B., 2004. Cave characteristics and speleothems in Xueyu Cave group, Fengdu, Chongqing city. Carsologica Sin. 23, 85–90 in Chinese with abstract in English.